UC San Diego

UC San Diego Electronic Theses and Dissertations

Title

Continuous Non-Invasive Arterial Blood Pressure Measurement Using Photoplethysmography

Permalink

https://escholarship.org/uc/item/8fq5k1hp

Author

Gunasekaran, Venmathi

Publication Date

2013

Peer reviewed|Thesis/dissertation

eScholarship.org Powered by the California Digital Library
University of California

UNIVERSITY OF CALIFORNIA, SAN DIEGO

Continuous Non-Invasive Arterial Blood Pressure Measurement Using Photoplethysmography

A Thesis submitted in partial satisfaction of the requirements

for the degree Master of Science

in

Bioengineering

by

Venmathi Gunasekaran

Committee in charge:

Jeffrey H. Omens, Chair
David A. Gough
Vishal Nigam
Guy P. Curtis

2013

The thesis of Venmathi Gunasekaran is approved, and it is acceptable in quality and form for publication on microfilm and electronically:

Chair

University of California, San Diego

2013

To Amma, Appa and Shiva for being my friends, philosophers and guides at all times.

In all chaos there is a cosmos, in all disorder a secret order.

- ***Carl Jung***

TABLE OF CONTENTS

LIST OF ABBREVIATIONS

PPG – Photoplethysmogram

NIBP – Non-Invasive Blood Pressure

CNAP – Continuous Non-invasive Arterial Pressure

SBP – Systolic Blood Pressure

DBP – Diastolic Blood Pressure

LIST OF FIGURES

ACKNOWLEDGEMENTS

In one's quest for order amidst the chaos in the universe, one always finds themselves receiving help, guidance and moral support from others. I came to UC San Diego to pursue my passion for developing medical devices and I would like to express my sincere gratitude to my adviser Dr. Jeffrey Omens, for his guidance and support, from the very beginning. This project is an initiative of Dr. Guy Curtis and Dr. Peter Tong and I would like to thank them for framing the problem statement and their suggestions on how I might proceed whenever I encountered hurdles. I would also like to thank Spacelabs Healthcare and Mr. Jeffrey Gilham for providing me with the equipment and for helping me understand their operation, at a very early stage in the project. Being a project that required statistical data analysis to judge the feasibility of the concept, collecting data from many subjects was a necessity. I extend my gratitude to Owen Huang and Jonathan Su for helping me with collecting data.

I thank my family for their ubiquitous moral support, even when half the planet separates me from them, and my friends- Roshni, Mukanth, Varsha and Amal for always lending a kind ear during murky times.

ABSTRACT OF THE THESIS

Continuous Non-invasive Arterial Blood Pressure Measurement using Photoplethysmography

by

Venmathi Gunasekaran

Master of Science in Bioengineering

University of California, San Diego, 2013

Professor Jeffrey H. Omens, Chair

Arterial Blood Pressure is one of the primary indicators used to monitor health. It is often useful to continuously observe fluctuations in the systolic and diastolic blood pressure in post-operative patients. Conventional devices like a sphygmomanometer are non-invasive methods of reading blood pressure, but are not continuous. Another commonly used technique, which is invasive, is an intra-arterial blood pressure sensing mechanism. A non-invasive method to continuously track variations in blood pressure is very useful as it has the advantages of not being

intrusive and hence eliminating the need to surgically implant a device to sense intra-arterial pressure and the risk of infection.

In this project, different methods of processing the photoplethysmogram signal are analyzed with the aim of identifying the components of the signal that vary with blood pressure, and can distinctly report the systolic and diastolic values. The data collected from 20 subjects is statistically analyzed. Pressure was also calculated from measured photoplethysmogram, using principles from photonics and biomechanics. This method was found to be the closest approximation to real-time pressure.

Analysis of different parameters of the photoplethysmogram indicates that even though it depends upon pressure to a certain extent, there is no simple relationship that is valid or consistent over a reasonable period of time. However, with some improvements to the sensitivity of the device and by using the calculated pressure from the photoplethysmogram, the real-time blood pressure can be measured.

Chapter 1: Introduction

Blood pressure, which indicates the force exerted by the blood flowing through our blood vessels on the arterial walls, is a critical parameter used to monitor health. Deviations from its normal level can be indicative of a plethora of disease conditions including heart disease, kidney failure, diabetes, hypertension and stroke [1]. Moreover, high blood pressure can lead to the bursting of blood vessels and hemorrhages while very low blood pressure causes dizziness and even loss of consciousness [2], [3]. If left untreated, high blood pressure can also lead to stroke, enlarged heart, heart attack, haemorrhages in the eye blood vessels and even peripheral vascular disease which leads to lack of blood circulation in the legs, cramp-like pain in the calves (claudication), or aneurysms. In addition, it is vital to monitor the blood pressure of peri-operative patients to ensure they're stable before and after surgery. [3]

The oxygen content of blood is another crucial parameter to determine good health. In healthy patients, the oxygen saturation, called SpO_2, is between 98 and 100%. This can be measured using a non-invasive clip-on device called a finger oximeter, which measures the amount of light of specific frequencies (in the red and infra-red regions of the spectrum) to calculate the amount of oxygen present. The finger oximeter typically has two light-emitting-diodes (LEDs) which emit specific frequencies of light, and two photodiodes, which measure the light transmitted through the finger by converting energy from the photons to voltage.

Figure 1.1 Finger Oximeter: Nellcor OxiMax SpO2 Finger Sensor [4]

The graph obtained by plotting the electric signal generated by the photodiode is called a photoplethysmogram (PPG). A normal PPG signal looks as shown in Figure 1.2. As can be seen, the amplitude of the signal varies as blood pulsates through the finger.

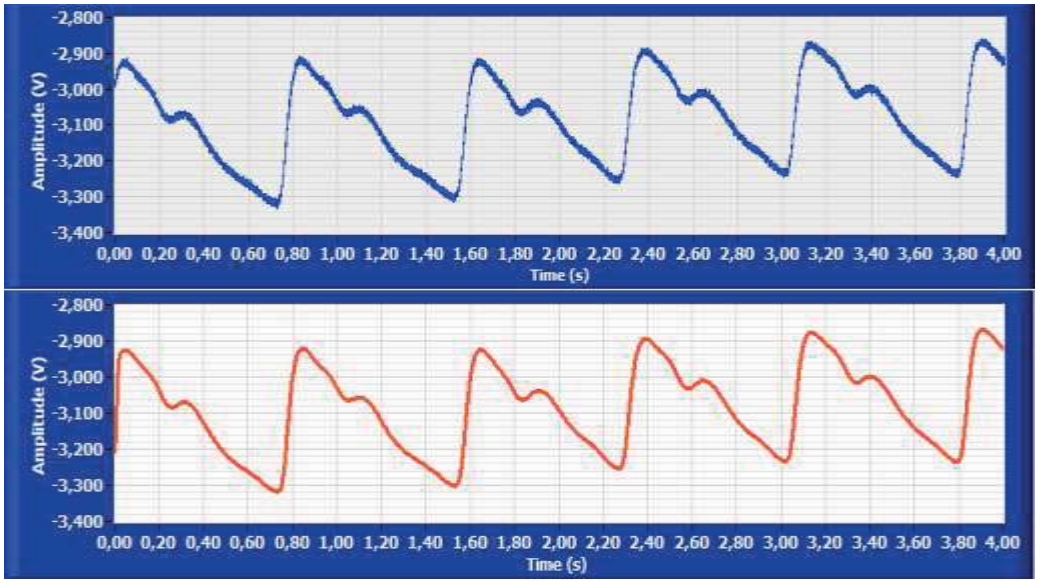

Figure 1.2 PPG. The blue curve on the top represents the Infra-red waveform and the red curve represents the "Red" light waveform [5]

The motivation behind this project is to use the PPG signal to attempt to infer the blood pressure, non-invasively and continuously. The PPG waveform was chosen because it has been observed that a patient's PPG disappears when an external cuff is inflated, while measuring blood pressure using a conventional Sphygmomanometer, and the signal reappears when the pressure in the cuff decreases. The aim of this project is to improve the presently available devices, designing a Continuous Non-invasive Arterial Pressure (CNAP) monitor that uses similar principles of PPG and minimize the need for an external cuff is the aim of this project. In addition to processing the non-invasive signal to display a real-time arterial blood pressure, modifying such a device, if feasible, to be insensitive to movement so as to be used on tilt-table tests in hospitals is a future goal of this project.

Chapter 2: Background

2.1 The Cardiac Cycle

The heart and the blood vessels constitute the human cardiovascular system and are primarily responsible for all transport within the body, including blood gases, nutrients from food, drugs, etc. The heart's pumping mechanism, which is a result of the rhythmic contraction and relaxation of its muscles, forms the driving force behind this transportation mechanism.

The cardiac cycle comprises five different stages, beginning with the "early-diastole" when the blood from the two atria passively flow into the two ventricles, while the semi-lunar valves (of the superior vena cava and the pulmonary vein) remain closed. In the next stage, the atria contract and forcibly drain all the blood in them into the ventricles. This is called "atrial systole". After this step, the two atrio-ventricular valves close and "iso-volumic ventricular contraction" occurs- which is when the ventricles begin to contract and pump blood into the aorta and pulmonary artery. In the fourth stage, also known as "ventricular ejection", the ventricles are contracting and empty and the semi-lunar valves of the aorta and pulmonary artery are open. During the fifth stage, "iso-volumic ventricular relaxation," no blood enters the ventricles. They stop contracting and begin to relax, and the semilunar valves close due to the back-pressure of blood in the aorta. The five stages of the cardiac cycle are illustrated in Wigger's diagram in Fig 1.1. It is important to note how the cardiac cycle is reflected in the aortic pressure curve, as the pressure in the aorta is the same pressure that is transmitted to the rest of the body.

pressure curve, as the pressure in the aorta is the same pressure that is transmitted to the rest of the body.

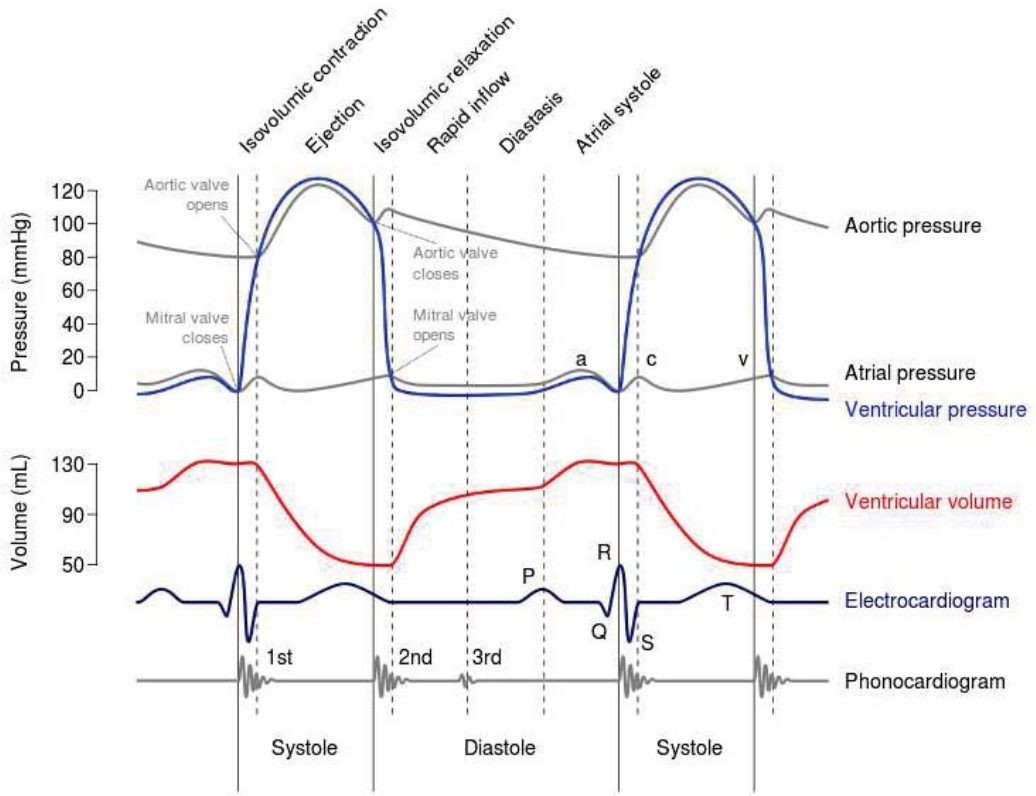

Figure 2.1 Wigger's Diagram [6]

2.2. Origin of blood pressure

Blood pressure is typically written as 120/80 mm of Hg. The higher value, called the systolic blood pressure (SBP) is the maximum pressure that is exerted by blood on the arterial walls. This occurs when the left ventricle pumps blood into the aorta, and the pump pulsates down to different parts of the body. The lower value of blood pressure, called the diastolic blood pressure, represents the minimum pressure that is always exerted by residual blood present in the blood vessels on the arterial walls. This

is the reading corresponds to the blood flow from the atria to the ventricles. However, there is a time delay between the actual blood-flow into the ventricles to the time when this is reflected in the arteries in other extremities of the body, from where the pressure is being monitored.

Normal systolic blood pressure falls in the range of 90-120 mm of Hg and the diastolic blood pressure, typically, lies between 60-80 mm of Hg. A variety of parameters including age, weight, and general metabolism affect the normal values of blood pressure. In general, systolic blood pressure increases with age and changes drastically over short intervals of time whereas the diastolic blood pressure changes at a much slower rate.

2.3 Photoplethysmography

Photoplethysmography is the volumetric measurement of an organ using light. A PPG (PPG) is obtained using a pulse oximeter which illuminates the skin and measures changes in light absorption. A conventional pulse oximeter monitors the perfusion of blood to the dermis and subcutaneous tissue of the skin. With each cardiac cycle the heart pumps blood to the periphery. Even though this pressure pulse is damped by the time it reaches the skin, it is enough to distend the arteries and arterioles in the subcutaneous tissue.

If the pulse oximeter is attached without compressing the skin, a pressure pulse can also be seen from the venous plexus, as a small secondary peak. The change in volume caused by the pressure pulse is detected by illuminating the skin with the light from a light-emitting diode (LED) and then measuring the amount of light either transmitted or reflected to a photodiode. Each cardiac cycle appears as a peak, as seen

in the Fig 2.2. Since blood flow to the skin can be modulated by multiple other physiological systems, the PPG can also be used to monitor breathing, hypo-volemia, and other circulatory conditions. Additionally, the shape of the PPG waveform differs from subject to subject, and varies with the location and manner in which the pulse oximeter is attached.

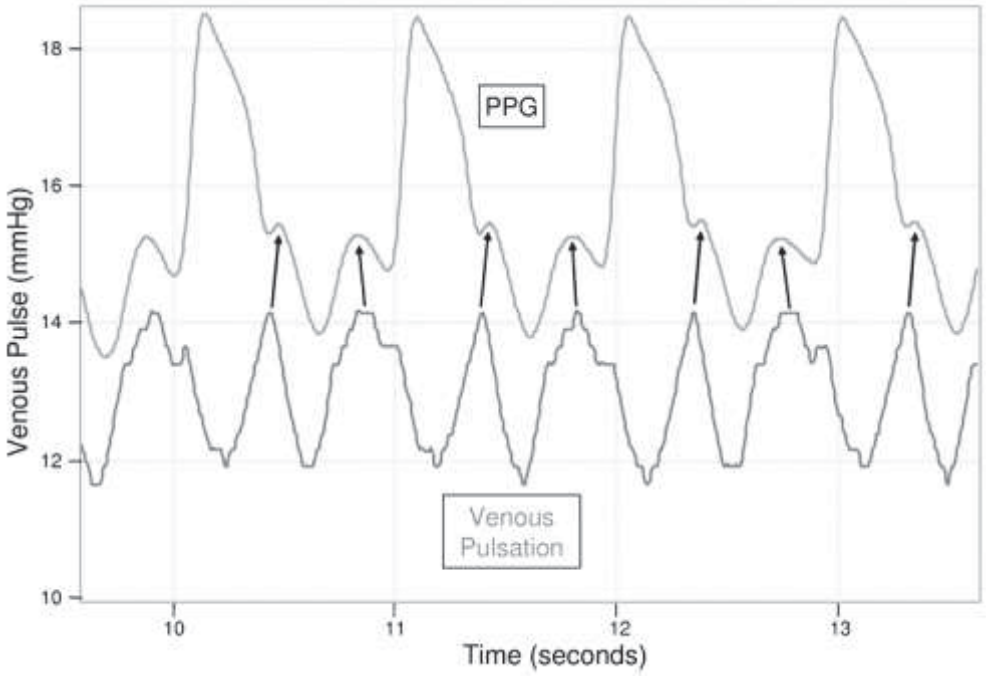

Figure 2.2. PPG (PPG) showing venous pulsations [7]

The PPG waveform has a fixed component and a varying component. The fixed component (or the DC component) is determined the amount of light absorbed by the different layers of the subject's skin. The varying component depends upon the volume of blood flowing through the blood vessels. The varying component (AC component) of the PPG has the same frequency of heart rate. [8] It rides on the fixed component and when the artery distends due to greater blood flow, there's a peak in the PPG. A smaller peak is seen when the blood flows back to the heart via the veins.

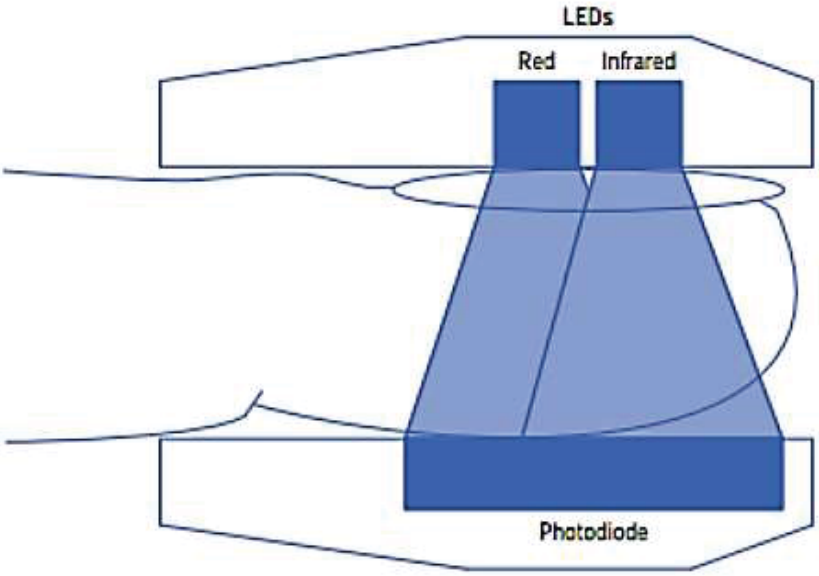

Figure 2.3 Schematic of finger pulse oximeter probe [9]

When light passes through the finger, blood absorbs a certain portion of it. Thus, the light transmitted to the photodetector can be calculated using Beer-Lambert Law, which is given by the following equation. [10]

$$A = \varepsilon . l . c = \log\left(\frac{I}{I_o}\right) \quad (1)$$

Where A is the absorbance of substance through which light passes, l is the length of the path, c is the concentration of the substance and ε is the constant of proportionality that relates absorbance linearly to l and c. I is the intensity of light that is transmitted and I_o is the intensity of light transmitted when the concentration of the absorbent is zero. The Beer-Lambert law helps us relate blood volume, or more precisely, the change in blood volume with the PPG signal.

The PPG signal, however, is very noisy and highly sensitive to movement. Several groups have been working on processing the signal to be movement insensitive.

[11] In addition, it is susceptible to erroneous readings when the perfusion is low. Such situations occur when vasoconstriction occurs- for example, when the limb or extremity on which the sensor is placed is cold. Nonetheless, the signal is very informative, if read when the device shows a steady pulse.

Figure 2.2 shows Premature Ventricular Contractions (PVCs), which can be identified by the characteristic presence of the ventricular-back-flow pulse before the main systolic peak. Ventricular tachycardia and ventricular fibrillation can also be detected using a finger-based PPG.

Chapter 3: Continuous Non-invasive Arterial Pressure Measurement- A Review

3.1 A Brief History of CNAP

Prior to the 19th century, circulatory health was assessed by sesnsing arterial pulses using palpitation. In 1816, the invention of stethoscope led to the development of the auscultatory detection of pulse by René-Théophile-Hyacinthe Laennec. [12] In 1835, Jules Hérisson developed a mercury based device to measure pulse pressure. [13] However, it was Poiseuille who developed the first hemodynameter, which could monitor blood pressure continuously. [14] Later that century, Karl von Vierordt and Étienne-Jules Marey independently developed a graphical device which could continuously plot the pulse pressure. [15], [16]

The most commonly used method to measure blood pressure in clinics is a sphygmomanometer. The most widely used version of this device comprises an external cuff, a mercury manometer and a stethoscope. [8] This was first developed by Italian scientist Scipione Riva-Rocci, in 1896, when he used a mercury sphygmomanometer along with palpation to measure the absolute systolic blood pressure. [17] A few years later, in 1905, Nikolai Sergejev Korotkoff discovered the Korotkoff sounds and thus, physicians were able to measure the absolute diastolic pressure too, using the upper-arm cuff method that Riva-Rocci introduced. [18]

Typically, the clinician wraps the cuff around the patient's upper arm and inflates it to a pressure of about 140-170 mm of Hg. When the cuff pressure is higher than the systolic blood pressure value, the brachial artery is completely occluded and

there is no blood flow. The clinician uses the stethoscope to listen to blood flow right below the patient's elbow, while slowly deflating the cuff, thereby decreasing the pressure exerted by the cuff on the patient's arm. When the pressure reaches the systolic blood pressure, Korotkov sounds can be heard. [19] Korotkov sounds represent the blood flow through an occluded artery. These sounds vanish when the cuff pressure falls below diastolic blood pressure, when the artery is fully open and blood flows freely. The pressure range between the systolic and diastolic points is called the Auscultatory Gap (Figure 3.1).

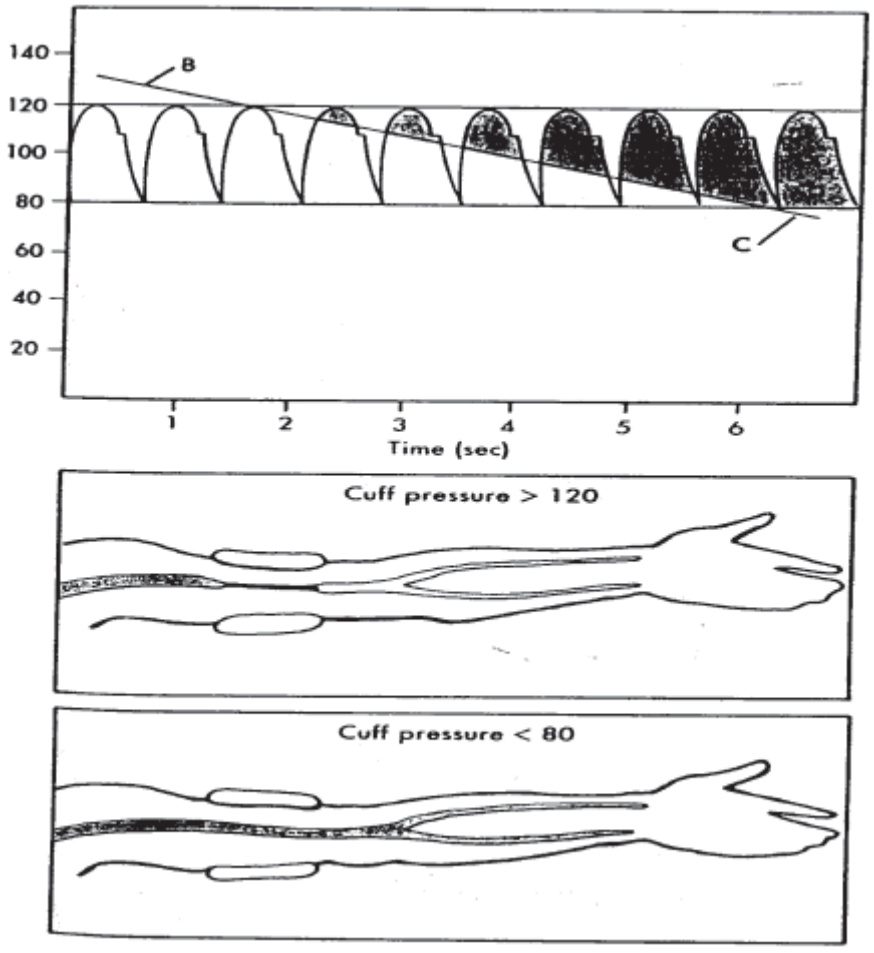

Figure 3.1 Conventional Sphygmomanometer using Auscultatory gap to measure blood pressure [19]

This method is robust and accurate. However, it gives us a point-measurement only and hence, cannot be used as an indicator of fluctuations in blood pressure. Making such measurements frequently results in soreness of the subject's arm. In addition, this technique is largely subject to human errors. A schematic of this technique is shown below, where the patient's blood pressure is 120/80 mm of Hg.

To continuously monitor the arterial pressure, an intra-arterial line is often placed in the patient during surgery. An intra-arterial line or an art-line is an inflatable catheter, which is usually placed in the radial artery (at the patient's wrist). The catheter has a pressure sensor which continuously reads the pressure exerted by blood on the arterial walls. This is, till date, the most accurate method of constantly observing changes in the blood pressure. However, inserting the catheter is often painful and is done with the patient under anesthesia. In addition, such invasive methods expose patients to risk of infection. To avoid this drawback of the art-line, several teams have been working on developing a device that will help us achieve similar results non-invasively.

Such Continuous Non-invasive Arterial Pressure (CNAP) monitors available in the current market use a volume-clamp method which employs a feedback loop and a servo control system to maintain the volume of the blood vessels in the finger placed in the sensor, a constant. This method was developed by Penaz. [20] A schematic of this technique is shown in Figure 3.2.

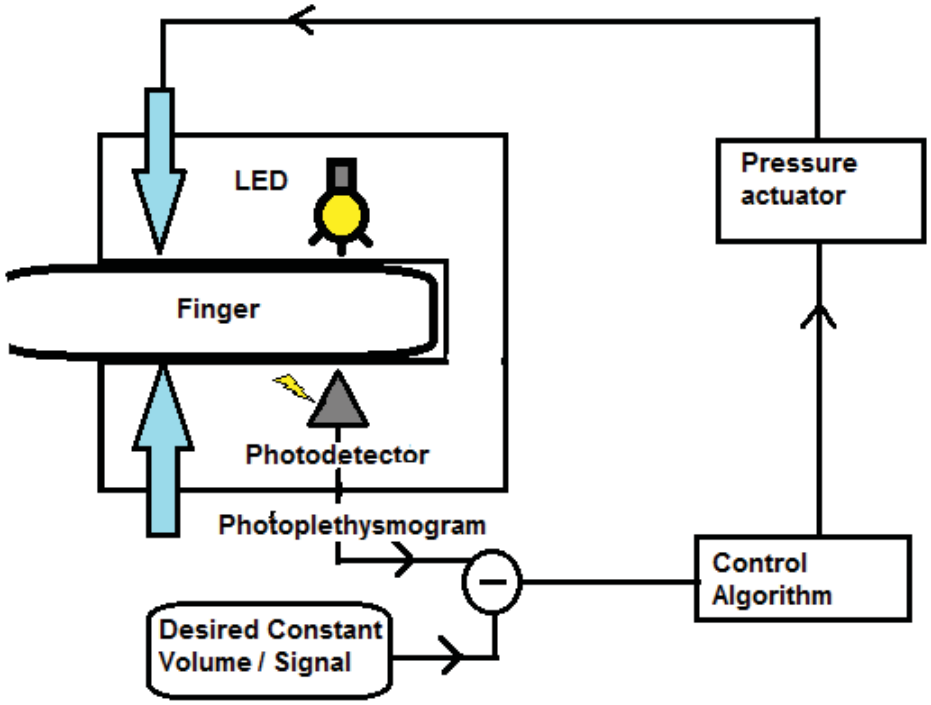

Figure 3.2. Schematic of the Volume Clamp method used for continuous and non-invasive blood pressure monitoring based on Penaz's technique [20]**,**

Here, the volume is maintained a constant by exerting pressure on the finger. Since the volume is constant, the changes in the pressure in the artery, also known as the pulse pressure variation (PPV), can be determined using the changes in the external pressure required to maintain the volume constant.

An Austrian research group, CNSystems, works on improving the vascular unloading technique to measure BP continuously. Their technique is based on the Penaz principle [20] where light from one or two sources is passed through a limb, finger, wrist, temple or a toe of a human subject and the light that is transmitter (as in the case of finger, toe, limb) or reflected (as in the case of temple or wrist) is used to record a PPG signal, using a photodetector, as previously described. The mean value is subtracted from the PPG obtained and fed into a controller. The control signal is

amplified and added to a set point pressure, which is then supplied to the cuff which encloses the body part used to measure the PPG from. When the heart pumps more blood into the blood vessels, the amplitude of the signal is higher. Hence, the control signal will also be higher, which results in a higher pressure being applied to the limb, that results in more blood being pushed out of the area being monitored, thereby decreasing the amplitude of the PPG, again. The assumption they make is that the blood volume is directly indicated by the PPG. Also, according to Penaz, the set-point pressure represents the Mean Arterial Pressure (MAP). CNSystems employs a method that uses two fingers to make the measurement. The volume is maintained constant using the feedback mechanism on one finger and the second finger is used to monitor the pulse oxygen content. The effect of venous pulsations is identified by comparing the signals obtained from the two fingers and removed. [21] This method, however, is still uncomfortable, as a constant pressure is applied on the patient's finger and could result in uneasiness and numbness.

Another recently developed technique used to non-invasively measure blood pressure involves tonometry. Radial arterial tonometry is a technique where a hand-held pressure sensor, that employs strain gage pressure sensors, is placed over the radial artery by applying mild pressure, just sufficient to flatten the artery. The pressure sensors in the tonometer read the radial pressure directly. [22], [23] Though it is a more direct and non-invasive method of observing changes in arterial pressure, this technique also requires external pressure to be applied on the patient's wrist and can often cause discomfort, especially when pressure needs to be monitored over long durations.

Shaltis, et al, from Massachusetts Institute of Technology, Cambridge, have incorporated a height sensor into a finger oximeter to enable it to measure mean arterial

pressure in real time. [24] A MEMS (Micro-electro-Mechanical Systems) based accelerometer was used as the height sensor and it was placed in a Finapres finger oximeter. Though this device is very compact and claims to be accurate, it cannot be used in hospitals, for perioperative care of patients, as the subject has to keep the hand with the sensor/finger oximeter raised for this technique to work.

3.2 Motivation for the current project

From the shape of the PPG, it is quite apparent that the PPG is related to the arterial blood flow. However, no precise arterial blood pressure-to-PPG relationship is known. Also, the optical processes that produce the PPG signal are poorly understood and hence, there are several theories as to what the PPG waveform quantitatively represents. It is believed to be the change in blood volume by some researchers, [25] or relative blood volume [26], while others consider it as a means to measure blood flow through the vessels present in the region used to measure PPG, which in many cases is an extremity of the body (like fingertip, toe, pinna of the ear, etc.) where circulation is primarily achieved by capillaries. [27].

3.3 Specific Aims

The goal of the project, as previously mentioned, is to develop a technique that can be used to measure blood pressure continuously and non-invasively using the principle of photoplethysmography. As discussed in Section 3.1, although there have been several methods developed to monitor blood pressure using PPG, these techniques all rely continuously upon an external device, such as a cuff to maintain constant volume of the finger, or an accelerometer to measure the height at which the limb or

body part used to measure the PPG is held. This project targets using the PPG solely, to predict the systolic and diastolic values of blood pressure, with minimum calibration using an external device, thereby minimizing discomfort for the patient.

For this purpose, it is necessary to first identify the best method of processing the raw PPG signal obtained from the finger oximeter sensor. The next step is to monitor how the filtered signal varies with pressure applied. Since it is not possible to induce blood pressure changes in subjects without injecting drugs like epidurals, the subject is made to wear a pressure cuff, which on inflation reduces the blood flow, and hence, the pressure in the artery. This filtered signal, along with the blood pressure data, is then to be used to identify components of the PPG that correlate with the systolic and diastolic blood pressure and their degree of reproducibility and accuracy. Different components of the signal and its derivatives are to be processed to identify how each of them correlates with Systolic Blood Pressure, Diastolic Blood Pressure and (or) Mean Arterial pressure. In addition, the PPG signal obtained at rest is to be analyzed to discern the components that remain constant when the subject is still, with no external pressure applied to the subject's arm.

Chapter 4: Methods

As mentioned in the previous section, the prime aim of the project is to identify characteristics of the PPG that are indicative of blood pressure. For this purpose, PPG data was collected from 20 healthy subjects. An automated sphygmomanometer, or a Non-Invasive Blood Pressure (NIBP) device, from Spacelabs Healthcare was used to measure the blood pressure. The NIBP device is programmed to inflate the cuff to a high pressure (between 180 and 200 mm of Hg) and then deflate in steps of 8mm of Hg. At every step, the pressure is held constant for approximately 15s.

The photoplethysmograph used in the following studies is from Spacelabs Healthcare with a finger probe from Nellcor. The LEDs emit two different wavelengths – red light at 650nm and 940nm in the Infra-red region of the spectrum. The detector is a silicon based photo-diode, which generates a voltage if excited by specific frequencies. As blood pulsates through the finger in the blood vessels below the LED, part of the light is absorbed and the rest reaches the photodiode. The photodiode then generates a voltage proportional to the intensity of light reaching it. This is called transmittance photoplethysmography. An alternate design is one where the LED and the photodiodes are both on the same side of the finger and the photodiode measures the light reflected from the finger, called reflectance PPG. The voltage obtained from the finger probe, as mentioned earlier, consists of a fixed or DC signal, which depends on patient specific parameters like size of the finger, skin color, thickness of skin, etc. The alternating component (AC) of the signal represents the blood flowing through the

vessels beneath the sensor. In this project, a Nellcor transmittance type finger probe is used.

4.1 Filtering of Raw Data

The data recorded is typically an alternating sinusoidal-like waveform with a variable offset. In addition to the offset, 60Hz noise is sometimes present. Movement artifacts are a significant source of error in finger oximetry. To extract the desired waveform, the signal is typically filtered. The most common filter used for this application is a second order Butterworth filter.

In signal processing, all filters that have a finite-time response to a finite-time input are called Finite Impulse Response (FIR) filters. There are other filters, known as Infinite Impulse Response (IIR) filters which continue to respond to a finite-time or impulse input given to the filter, long after the input has ended. This continued response maybe due to internal feedback that continues to stimulate the filter. However, in practice, the impulse response of IIR filters decreases with time and eventually approaches zero. Butterworth filters, Chebychev filters and most analog filters are IIR filters. [28] A Butterworth filter is a type of discrete-time signal processing filter that has a flat response in the pass-band. A flat response in the pass-band ensures minimal attenuation in the frequencies that the filter allows to pass through it, as shown in figure 4.2. However, in practice, it is impossible to obtain perfectly flat responses, especially at frequencies closer to the corner frequencies of the pass-band. Nonetheless, Butterworth mathematically proved that a very close approximation could be achieved using higher orders filters, where the corner frequencies had minimal attenuation. [29], [28]

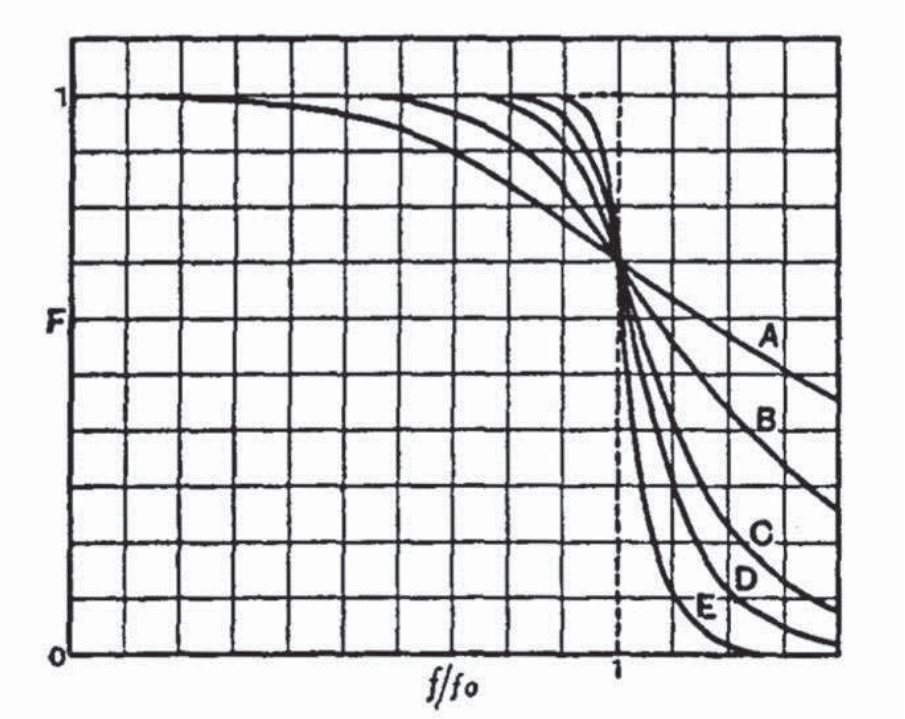

Figure 4.1. Output magnitude vs. frequency plots of filters designed by Butterworth. [29] **The curve labelled A represents the response of a first order filter, B - of a second order filter, C – fourth order, D – sixth order and E – eighth order filters. The dotted lines represent the ideal filter response. As can be seen, the filter response is closer to the idea filter as the order is increased.**

In Dolphin- the graphic user interface application developed by Spacelabs to filter and display the PPG, a second order Butterworth filter with corner frequencies of 0.01Hz and 2Hz was used. A lower order was chosen as the sampling rate of the signal is 27.5 samples/second, which is low.

However, as a higher order filter has better performance around the corner frequencies, a different filter was used. The raw signal obtained from the finger probe was filtered using an FIR filter which filters out the high frequency (greater than 10Hz) components of the raw data, leaving data which falls in the range of interest, around the range of heart rate. The DC component of the signal was filtered out using an IIR filter.

IIR filters can be unstable due to the nature of their response and positive internal feedback, whereas FIR filters are always stable. For this reason, they were used in combination here.

The raw data was fed to the FIR filter for removing the DC part of the PPG data as well as any high frequency (60Hz) noise that might have crept into the system. The filter used was a hamming window low-pass filter with order of 51, which provides a sharp cutoff at 10 Hz with steep attenuation of 50 dB. This filter was designed in MATLAB.

The DC component of the raw signal was removed using an IIR filter. The transfer function of the filter is:

$$H(s)=\frac{(1+s)}{(1+\alpha.s)} \qquad (1)$$

To obtain a DC attenuation of 22 dB, the value of α is at 0.992.

Another simple filter that was used was a DC offset filter. In this, the average value of the PPG signal over one cycle was found and subtracted from that cycle. The performance of the three different filters, programmed in MATLAB R2012b, is illustrated in chapter 5.

4.2 Experiments

Blood pressure and PPG/pulse oximetry data was collected simultaneously. This ensures that when the pressure in the cuff is high, the brachial artery would be occluded and the PPG would vanish. As the pressure in the cuff gradually decreases

below systolic pressure, blood starts trickling through the artery at low pressure. When the pressure further decreases below diastole, the artery opens fully and blood flows freely through it. Such an experiment is necessary to identify patterns, if any, in the variation of PPG signal with externally applied pressure, which in turn affects the blood flow within the artery, without artificially inducing blood pressure changes using drugs like epidurals.

However, since the pulse oximtery and NIBP devices used are both independent of each other, the foremost hurdle faced was time-synchronizing the two devices. Initially, it was proposed to introduce a sharp deviation in the cuff pressure, which would translate to a sharp change in the PPG signal. However, in most cases, disturbing the NIBP device, while it was in operation, gave erroneous pressure readings, often resulting in the device recalibrating itself. Hence, the NIBP program was manually started 10 seconds after the pulse oximeter started collecting data. Though this is not a precise method of synchronizing the two signals, it is adequate for this application, as the time difference between the signals was less than 1 second.

Initially, data was collected from subjects with their hand resting on a table, and the finger oximeter sensor placed at a level approximately at the same height as the subject's heart. This was done to avoid effects of gravitational force on the blood pressure at the finger-tip. However, this arrangement was later deemed unfit as there was a significant delay, of approximately 10s, between the point when the systolic blood pressure was reached and the pulse oximeter signal reappeared.

(a)

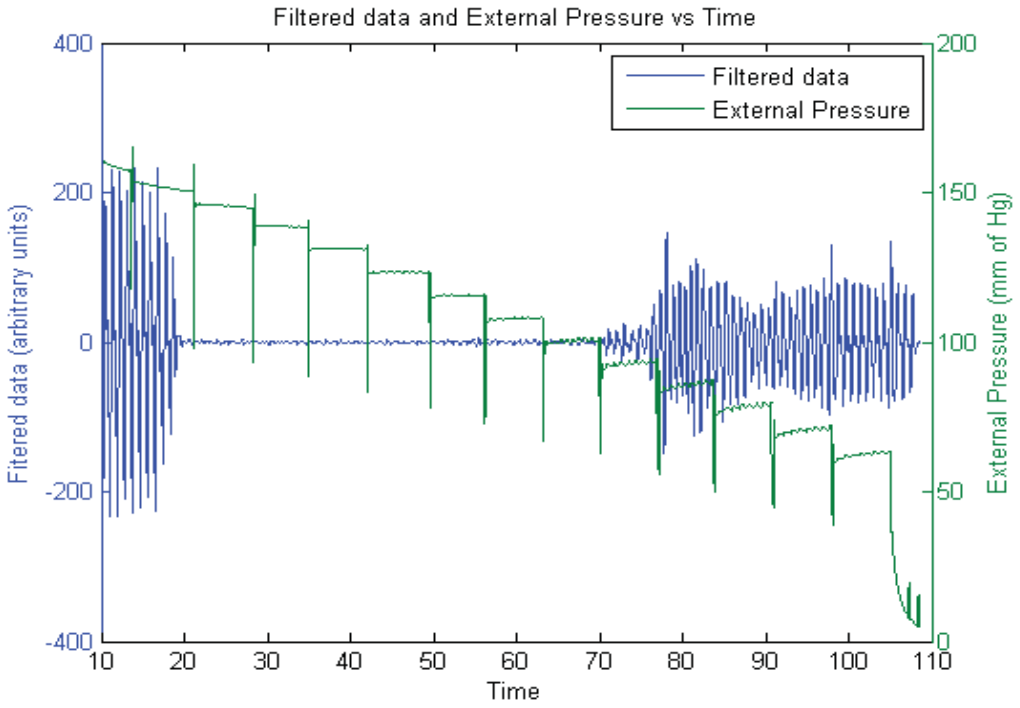

(b)

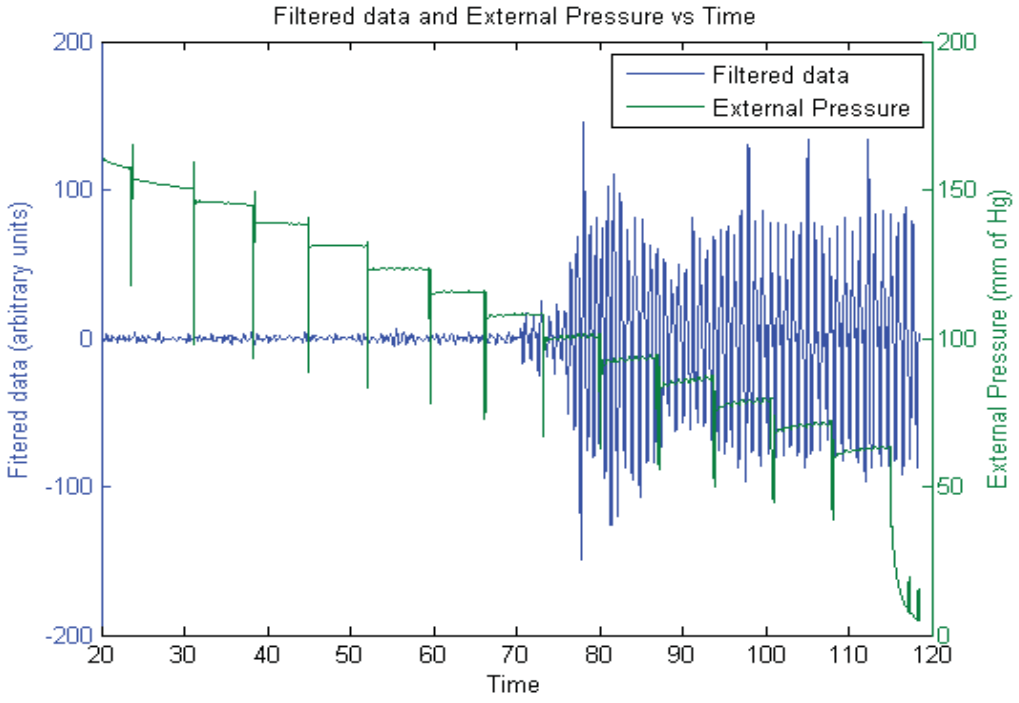

Figure 4.2 Pressure and filtered PPG amplitude vs. time when (a) subject's arm is placed horizontally on a table, at approximately the same level as subject's heart and when (b) subject's hand held vertically down. In both cases, subject's systolic blood pressure was 110mm of Hg and diastolic blood pressure was 70mm of Hg (±5mm of Hg)

As illustrated in figure 4.1(a), the systolic blood pressure is reached at approximately 55s, but the signal reappears only at 70s. However, when the subject's arm was held vertically down, the systolic blood pressure was reached at 65s and the signal reappeared at around 72s. To overcome the excess delay, blood pressure was measured with the patient seated, and arm hanging vertically down. Simultaneous pressure readings were taken manually, using a sphygmomanometer, while the NIBP device and pulse oximeter were in operation. In this method, gravitational force helps in reducing the delay and it was observed that the PPG signal reappeared within an average of 2 seconds after the cuff pressure fell below systolic blood pressure.

In addition to observing the PPG signal while the NIBP device was in operation, data was also collected from the pulse oximeter device while the patient was at rest. This was done to verify which components of the signal remain fairly constant over time. The assumption made here is that the pressure of a subject, when seated and at rest does not vary significantly with time.

4.3 Computing amplitude and slope

Among the parameters considered as possible indicators of blood pressure are the pulse amplitude of the PPG waveform and its slope. The amplitude was calculated by first filtering out the AC component, using the filter described in section 4.1 and then finding the maxima and minima using a peak detection algorithm. This algorithm is also used to store the time instances at which the above mentioned maxima and minima occurred.

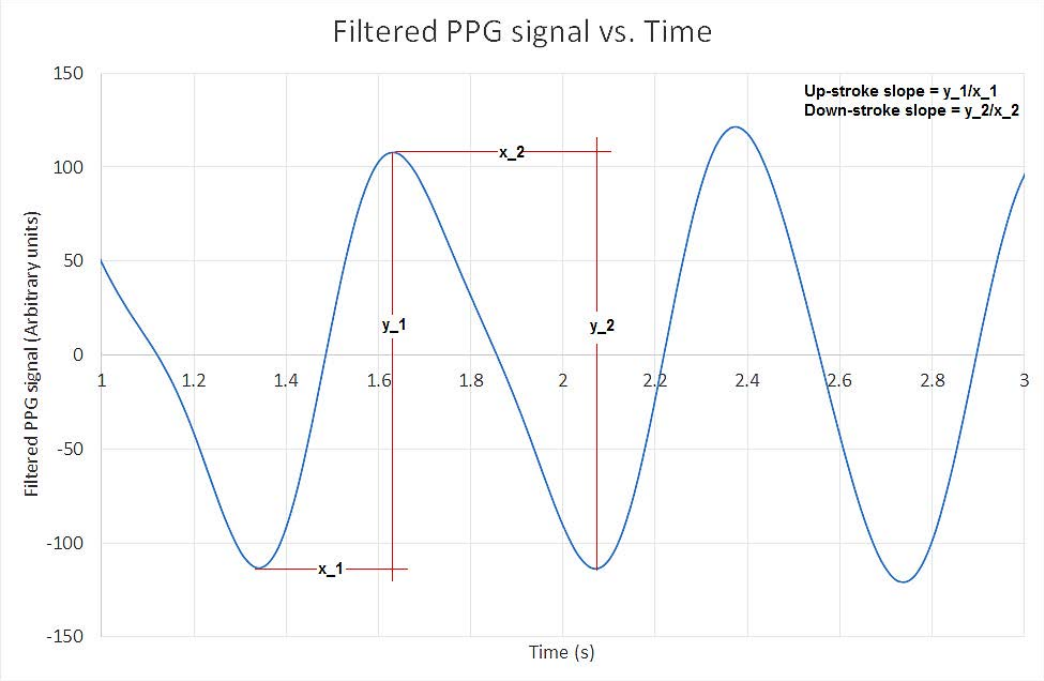

Figure 4.3 Illustration of the computation of up and down stroke slopes or velocities.

The average up-stroke slope is calculated by dividing the amplitude by the time taken for the signal to go from the previous minimum to the maximum. Similarly, the average down-stroke time is also calculated. Figure 4.3 illustrates this calculation.

4.4 Calculation of Blood Volume and Blood Pressure

As discussed in section 2.3, Beer-Lambert law governs the relationship between observed light intensity and volume of blood flowing in the region of the artery illuminated by the LED. This implies that the change in length l is directly related to the logarithm of the ratio of intensities – which are proportional to the voltage generated but the photodetector. Therefore,

$$l = -\frac{\log(\frac{I}{I_o})}{c.\varepsilon} \qquad (3)$$

In this equation, ε is a constant, for blood. In this case, c can also be considered constant as the oxygen saturation of blood in a healthy adult is roughly between 98 and 100% and since this value is relative (in %), it doesn't change with the volume of blood flowing through the artery. I is the intensity of light that is transmitted, which is measured in real-time by monitoring the voltage generated by the photodetector. I_o is the voltage generated due to parameters other than blood, i.e. the DC component of the PPG signal. This can be calculated by subtracting the AC component of the signal from the raw signal obtained from the photodetector.

Langewouters et al computed a relationship between the pressure exerted on the wall of an artery in the human finger and the change in the arterial radius [30], [31], [32]. The relationship obtained is as follows:

$$E = 2\frac{\Delta P}{\Delta d_e}(d_e^2 - d_i^2)(1 - \sigma^2)(d_i^2 d_e) \qquad (4)$$

E is the Young's modulus, σ is the Poisson's ratio (here, it is 0.5), d_i is the internal diameter of the artery and d_e is the external diameter. 'Δp' is the change in pressure and Δd_e is the change in diameter due to the exerted pressure. They also calculated the internal diameter di of the vessel, assuming constant wall volume V_w, as:

$$d_i^2 = d_e^2 - \frac{4.V_w}{\pi r^2} \qquad (5)$$

This can be substituted in (4) to get Δp in terms of Δd_e and d_e as can be seen in equation (6).

$$\Delta P = \Delta d_e\left(\frac{4\,V_w}{\pi r^2}\right)\frac{1}{2E(1-\sigma^2)\left(d_e^3 - \frac{4\,V_w}{\pi r^2}\right)} \qquad (6)$$

Notice that $d_e + \Delta d_e$ is the same as the path length *l* in Beer-Lambert's law. By combining the two equations, the pressure can be calculated from light intensity. From the expression, it is evident that the change in pressure is approximately directly proportional to the change in d_e or Δd_e. The pressure can be computed in real-time from the change in arterial radius using the relationship proposed by Langewouters et al, the change in pressure in an artery can be related to its change in radius and the change in radius is given by Beer-Lambert's law. The net equation is given below:

$$\Delta P = c.(log_{10}\left(\frac{I}{I_o}\right) - d_e)\left(\frac{4\,V_w}{\pi r^2}\right)\frac{1}{2E(1-\sigma^2)\left(d_e^3 - \frac{4\,V_w}{\pi r^2}d_e\right)} \qquad (7)$$

It must be remembered that this method involves many approximations, which may not be valid in practice. The extent to which this relationship can be used to assess pressure is discussed in Chapter 6.

Chapter 5: Observations and Results

5.1 Filter Performances

The figure below, Figure 5.1, shows the raw PPG data obtained for a period of 15 seconds. To identify the frequencies present in the signal, its Fast Fourier Transform and Power Spectral Density were plotted. As can be seen from Figures 5.2 and 5.3, there was only one dominant frequency and it matched the heart rate.

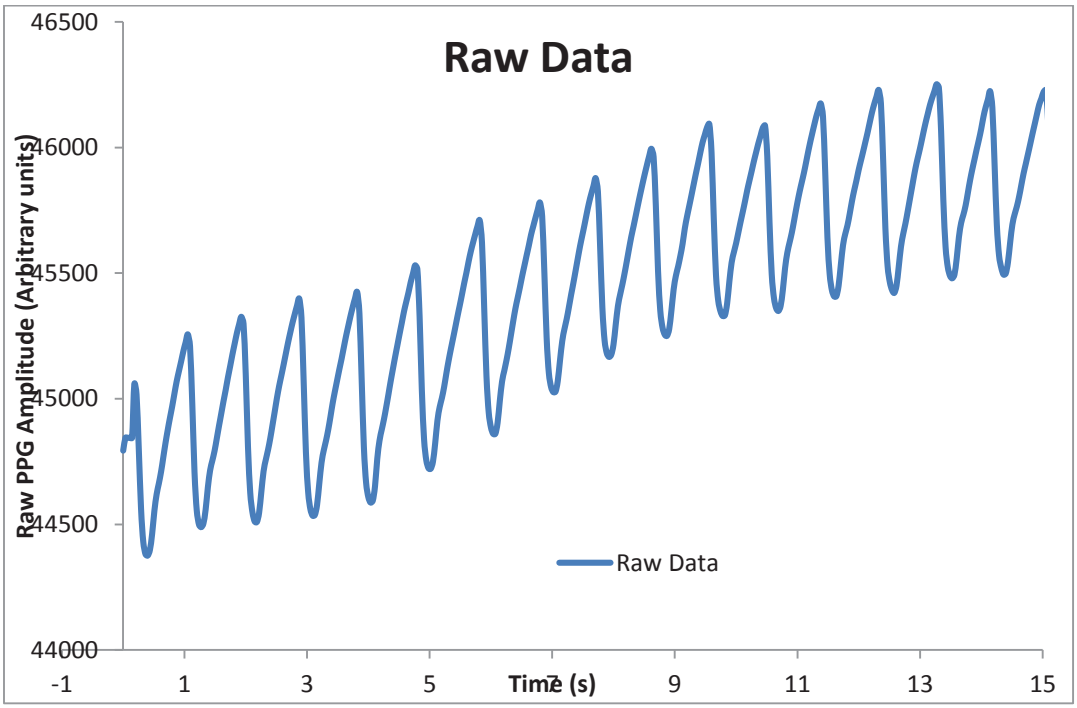

Figure 5.1 Raw PPG signal for a period of 15 seconds

To identify the frequencies present in this raw signal, a Fast Fourier Transform was performed on the data, using MATLAB. The Power Spectral Density was plotted too. The graphs showed a dominant frequency, which matched the heart rate. These plots helped determine the frequency range required to design the filter.

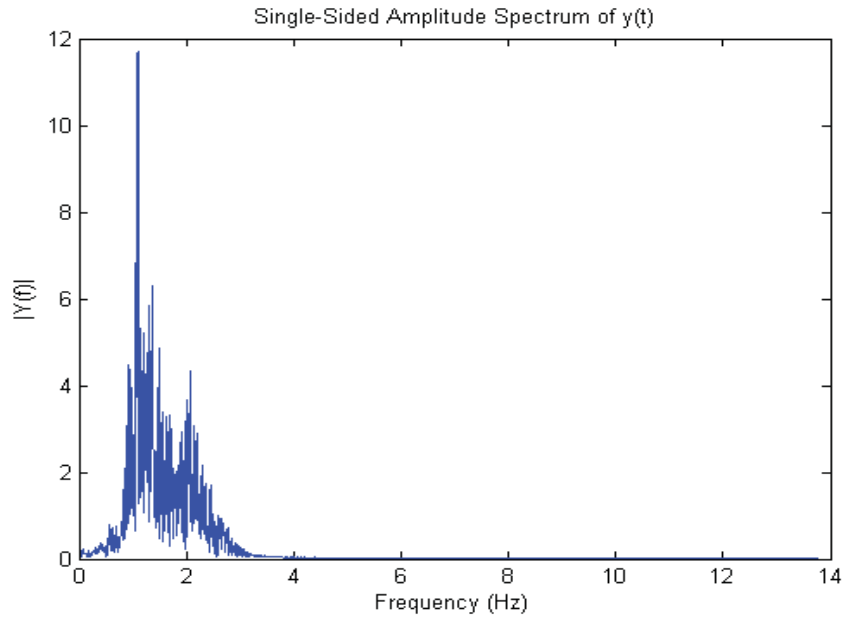

Figure 5.2. Fast Fourier Transform of the raw PPG showing a peak at approximately 1.2Hz

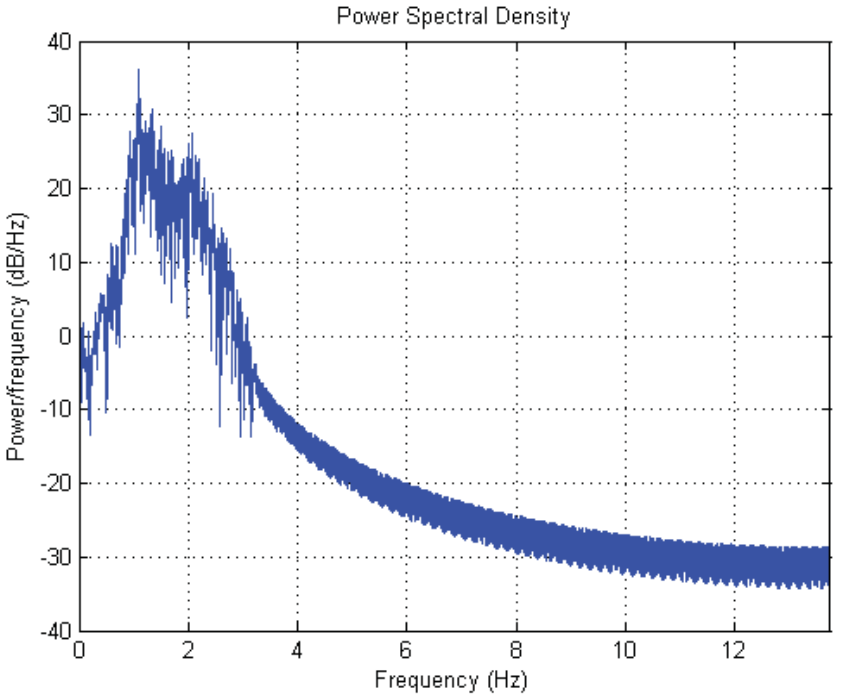

Figure 5.3. Power Spectral Density of the raw PPG, showing a peak frequency of approximately 1.2Hz

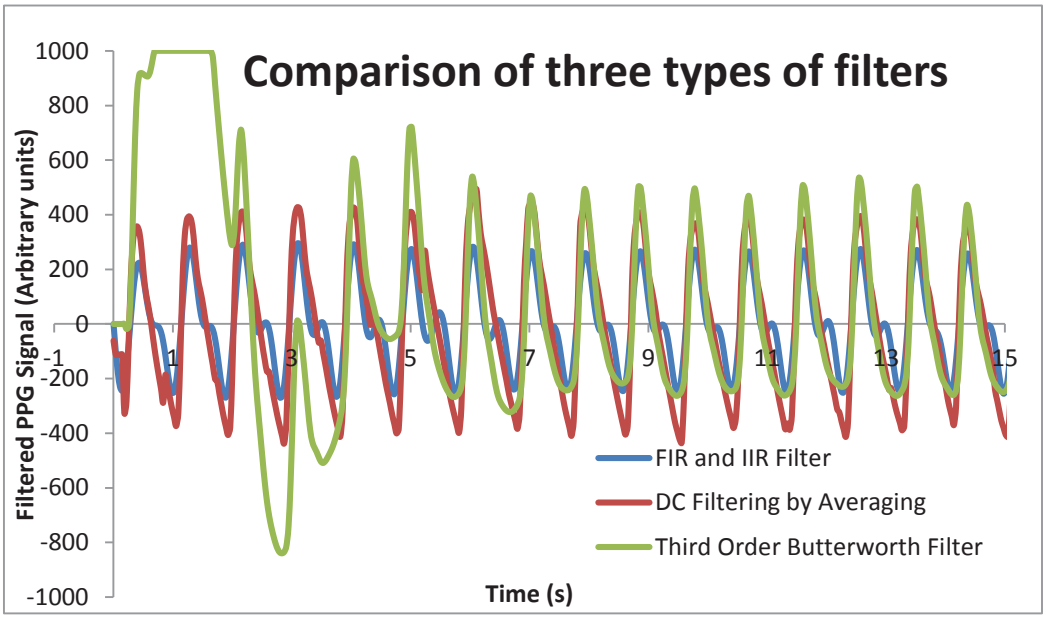

Figure 5.4 Comparison of the three different filters

Figure 5.4 shows the performance of the three different filters described in section 4.1. A filter is considered to perform well if it transmits the signal in the pass-band frequency range faithfully and dampens all other frequencies. In this case, performance criteria include removal of the DC component so that the signal is uniformly centered at zero, removes high frequency noise (like interference from nearby 60Hz sources) and removes the variation in PPG amplitude introduced due to breathing, all while retaining the shape of the signal in the pass-band. It can be seen that the third order Butterworth filter is highly noisy and unstable at the beginning. However, after about 2 seconds, it performs similar to the other two filters. As can be seen in the figure above, the FIR and IIR Hamming window filter is the one which retains the shape of the PPG most faithfully. However, when a device like the Spacelabs Pulse Oximeter with very low sampling frequency is used, a filter of such high order might not be necessary. The averaging filter performs very well in terms of removing the DC component and retaining the characteristic shape of the PPG waveform. But

when filtering the signal in real-time, it always lags behind by one cycle, as the processor needs values from one complete cycle to calculate the average DC value.

In all the experiments performed, the FIR Hamming window filter coupled with an IIR filter to remove the DC offset was used as it is shown to have much better stability, sharper roll-off at the corner frequencies and flatter pass-band.

5.2 Raw and filtered data at different external pressures

Preliminary analysis was done by plotting the raw PPG data and filtered data obtained from subjects at different values of external pressure. This was achieved by using a manual sphygmomanometer to hold the pressure on the subject's arm at a particular value, while simultaneously recording the pulse oximeter reading. The plots obtained are included in Figures 5.5 and 5.6. The systolic and diastolic blood pressures of each subject is given in Table 1 in the Appendix.

From Figures 5.5 and 5.6, it was evident that increase in external cuff pressure, or decrease in internal blood flow, affected the shape of the PPG. As a general trend, the PPG amplitude decreased with increase in pressure. However, this amplitude or the normalized amplitude - obtained by dividing the amplitude at any given pressure by the amplitude at zero pressure, did not follow a specific pattern, as can be seen in Figure 5.7.

Figure 5.5. Raw PPG data obtained from subjects when manually inflating a cuff to various values of external pressure

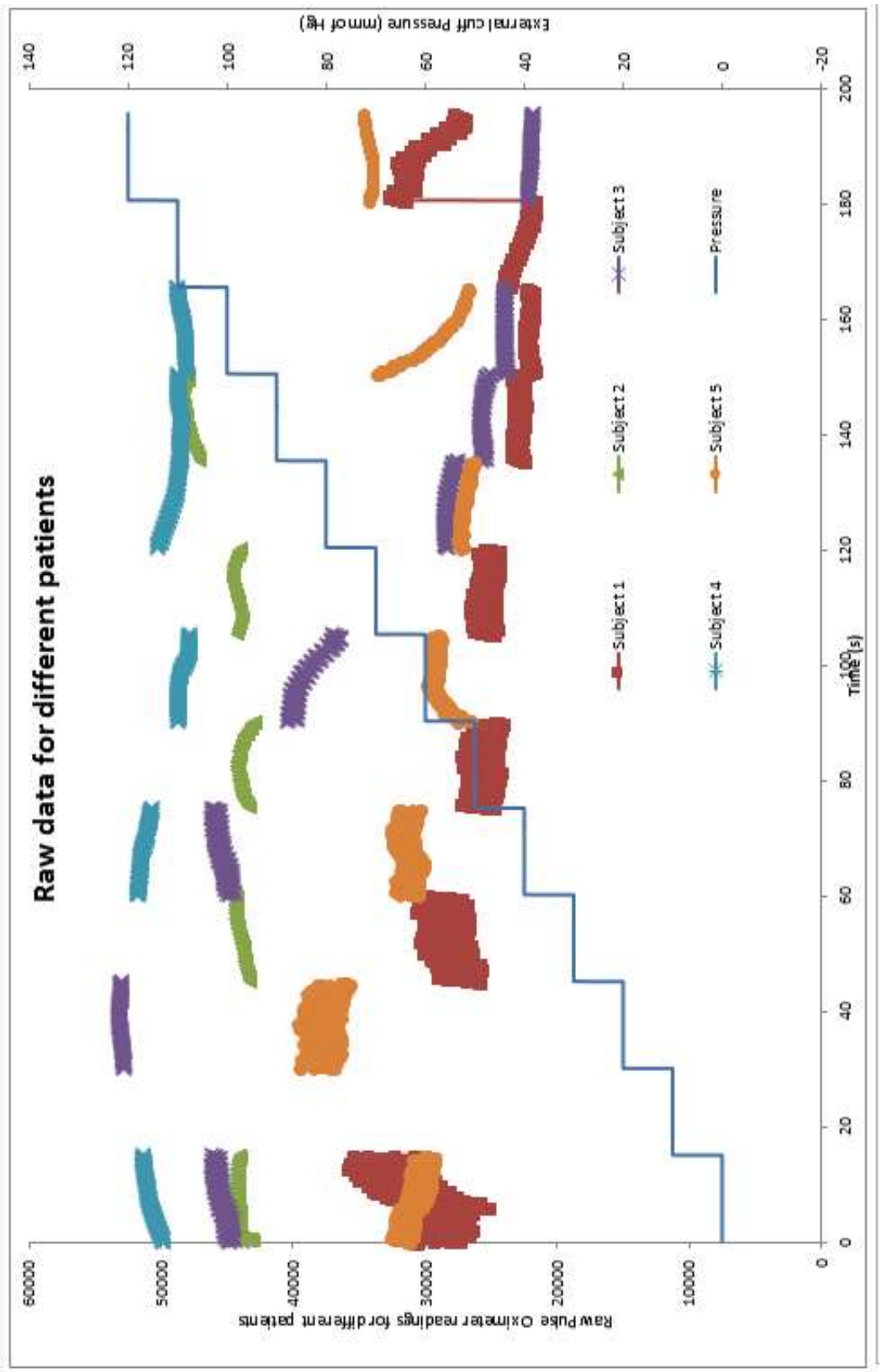
Raw data for different patients
Raw Pulse Oximeter readings for different patients
External cuff Pressure (mmof Hg)
Time (s)
Subject 1
Subject 2
Subject 3
Subject 4
Subject 5
Pressure
60000
50000
40000
30000
20000
10000
0
140
120
100
80
60
40
20
0
-20
0
20
40
60
80
100
120
140
160
180
200

Figure 5.6. Filtered PPG data obtained from subjects

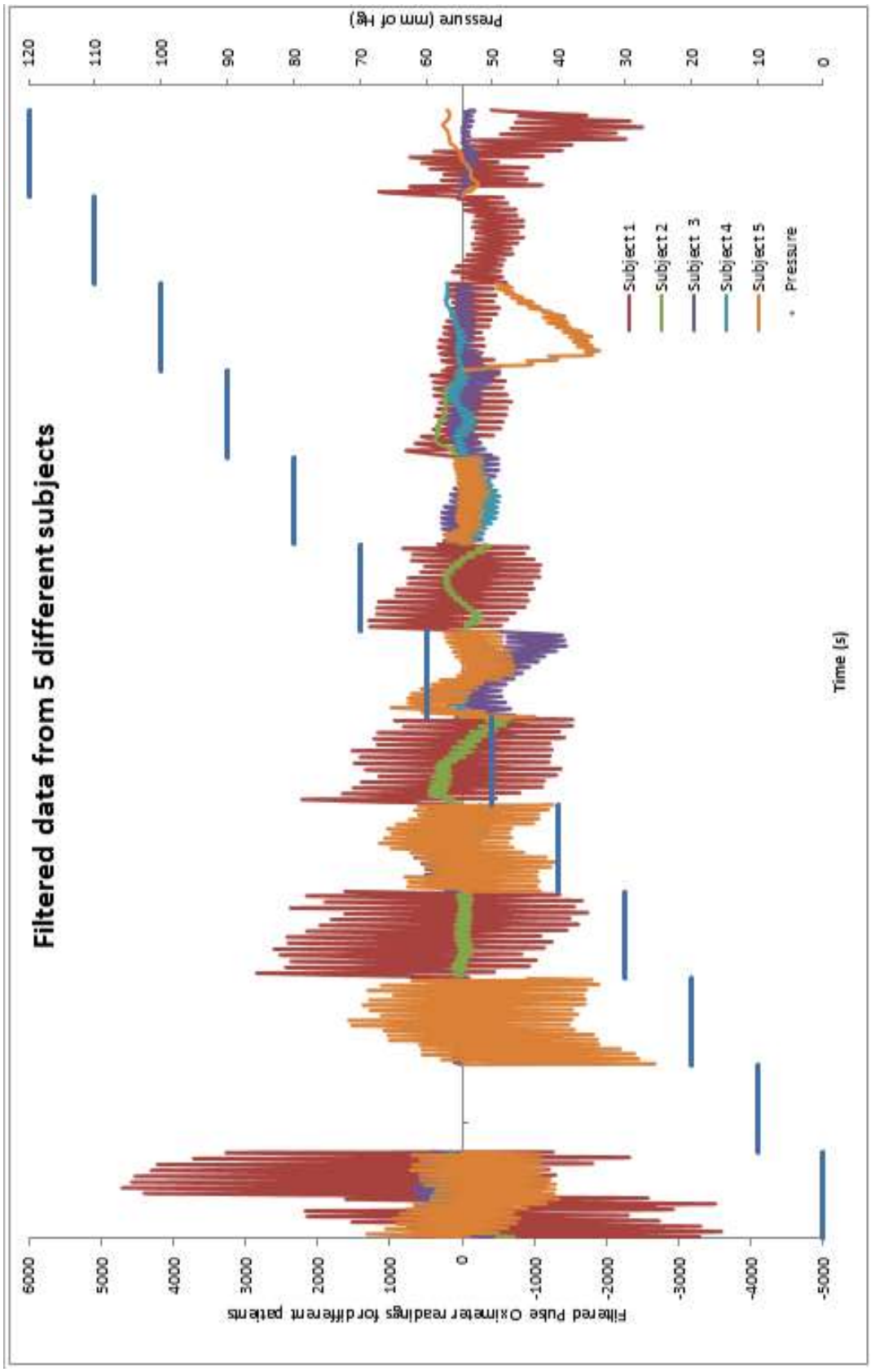
Filtered data from 5 different subjects
Filtered Pulse Oximeter readings for different patterns
Pressure (mm of Hg)
Time (s)
Subject 1
Subject 2
Subject 3
Subject 4
Subject 5
Pressure
6000
5000
4000
3000
2000
1000
0
-1000
-2000
-3000
-4000
-5000
120
110
100
90
80
70
60
50
40
30
20
10
0

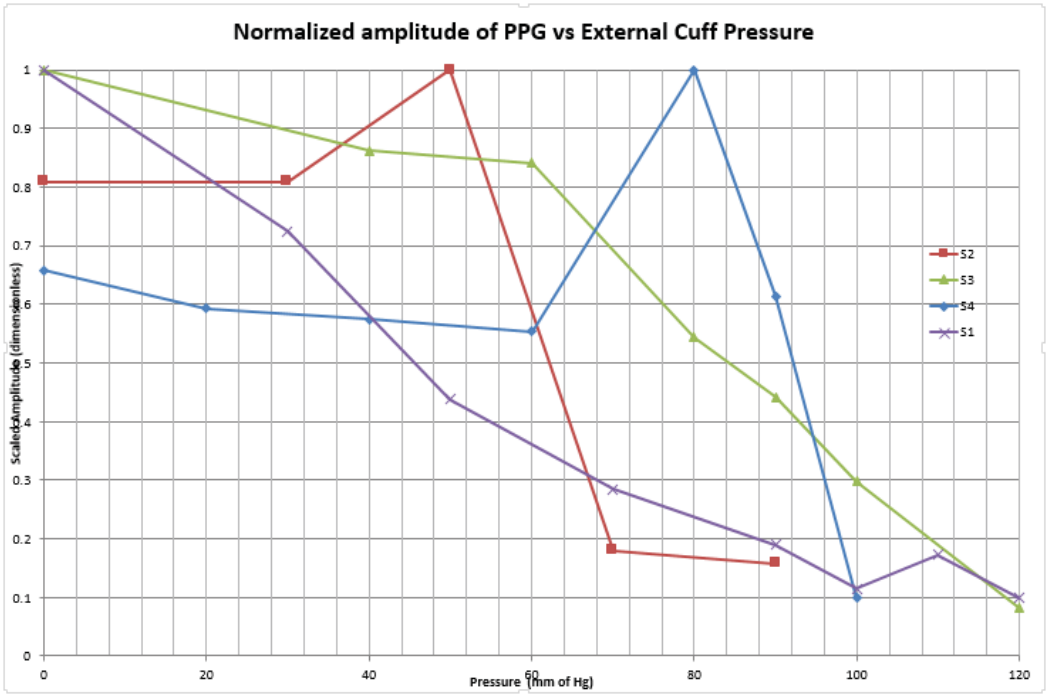

Figure 5.7. Normalized amplitude of PPG vs. Pressure for 4 of the subjects

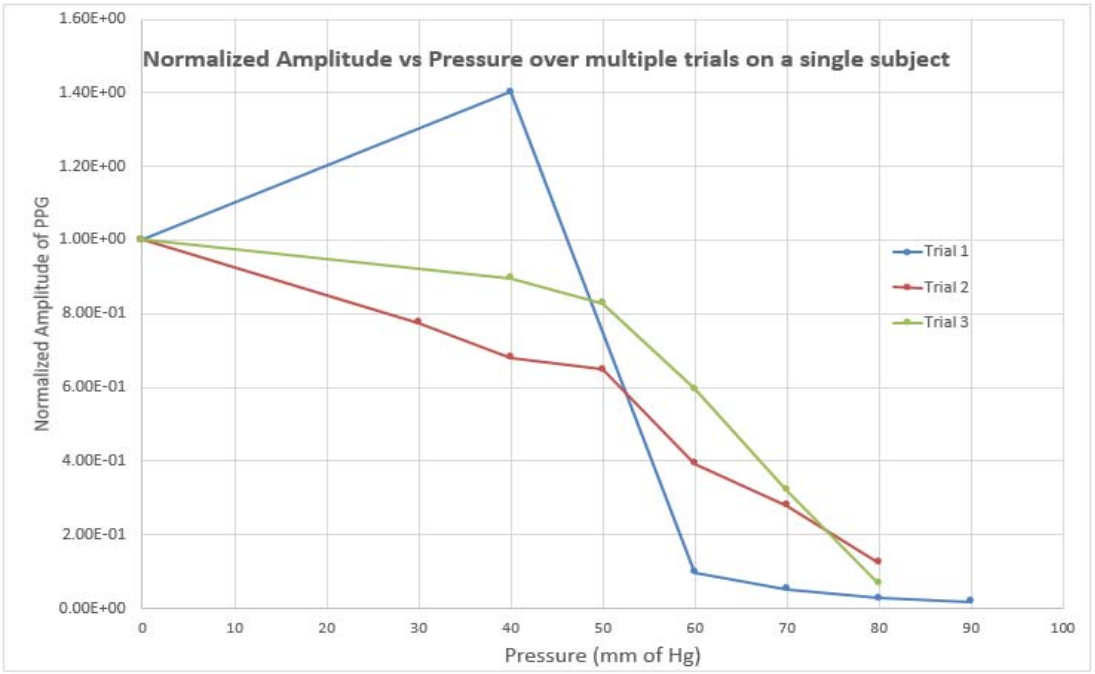

Figure 5.8 Normalized amplitude of PPG vs Pressure of the same subject, over multiple trials.

Figure 5.8 shows that the normalized amplitude vs. pressure curve obtained by manual measurement is not reproducible for the same subject. Moreover, while it is easy to identify the systolic pressure as the point where the normalized pressure is close to zero, it is difficult to identify the diastolic pressure. However, this was done manually, and hence, is a very rudimentary analysis, primarily because of its high susceptibility to manual errors. It is difficult to control the manual sphygmomanometer to maintain the cuff at the desired pressure over a long duration. Hence, the NIBP device from Spacelabs was used to apply pressure on the subjects' arm while the Spacelabs Pulse Oximeter kit simultaneously recorded the PPG. As described in section 4.2, when the subject's arm was horizontally placed, there was a large delay in the response of the PPG to an applied change in pressure, as depicted in Figure 5.9. In addition, it was observed that this delay decreased with decreasing external pressure.

To avoid this, the subjects were asked to hold their arms vertically down during the experiments. PPG data was collected from the subjects both when the NIBP device was in operation and while the subject was at rest.

This data from 20 subjects broadly fell into 3 categories. The amplitude of the PPG went to zero, or very close to zero) when the cuff pressure was raised to above systole and when the cuff pressure was decreased below systole, the PPG waveform reappeared, as expected. On further decrease in the cuff pressure, the amplitude and slope both either (a) increased till the diastolic pressure and then decreased, or, (b) uniformly increased between systole and zero pressure or (c) increased in amplitude from systole, experienced a dip in value of the amplitude/slope at diastole and then increased again. An example of each of these responses is included in the Figure 5.9 that follows.

(a)

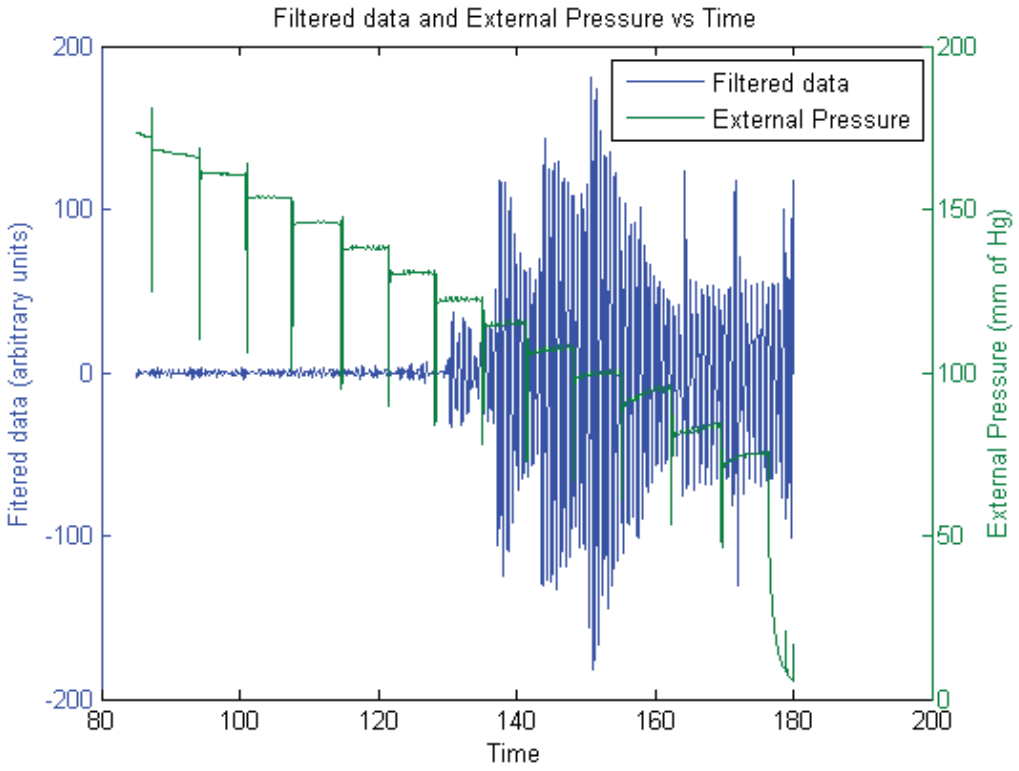

Figure 5.9. Plots showing different types of responses of PPG to the external pressure applied using the NIBP device. (a) shows the filtered data and external pressure versus time, (b) shows the change in amplitude with pressure and (c) and (d) show the down and down-slope of the data vs pressure. In all three figures, subject's SBP = 129mm of Hg, DBP = 84 mm of Hg. Similarly, (e) , (f), (g) and (h) show the data collected from a subject with SBP = 128mm of Hg and DBP = 80mm of Hg and (i), (j), (k) and (l) show the response of a subject with SBP = 103 and DBP = 68 mm of Hg. In all three cases, it can be seen that the pattern of the change in amplitude is not uniform. In addition, the average slope follows a pattern similar to the amplitude change but displays a sharp rise in magnitude just after systole and diastole.

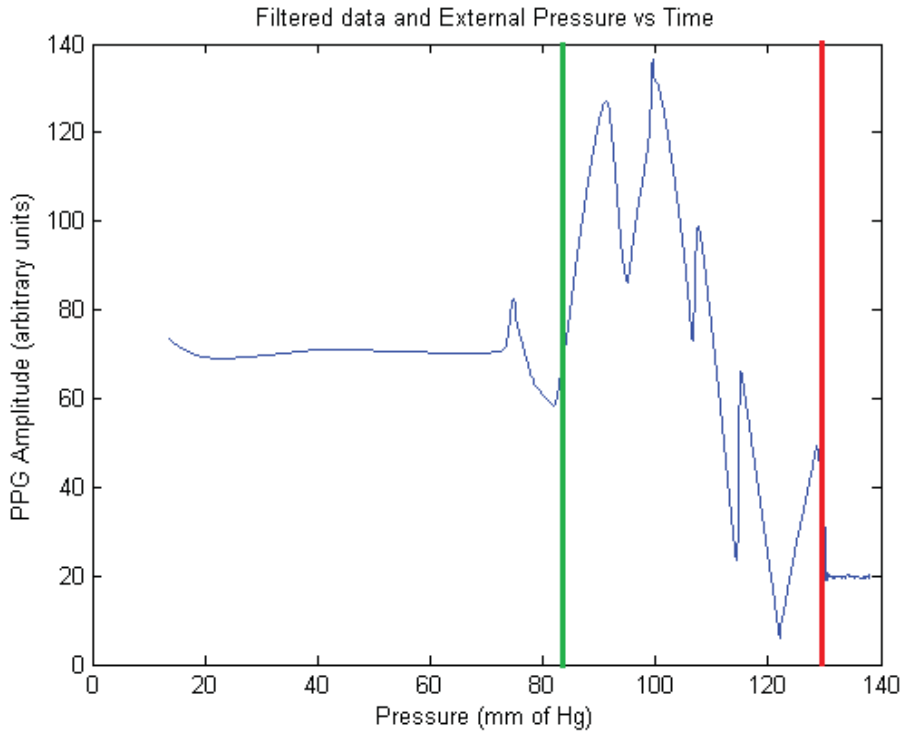

(b)

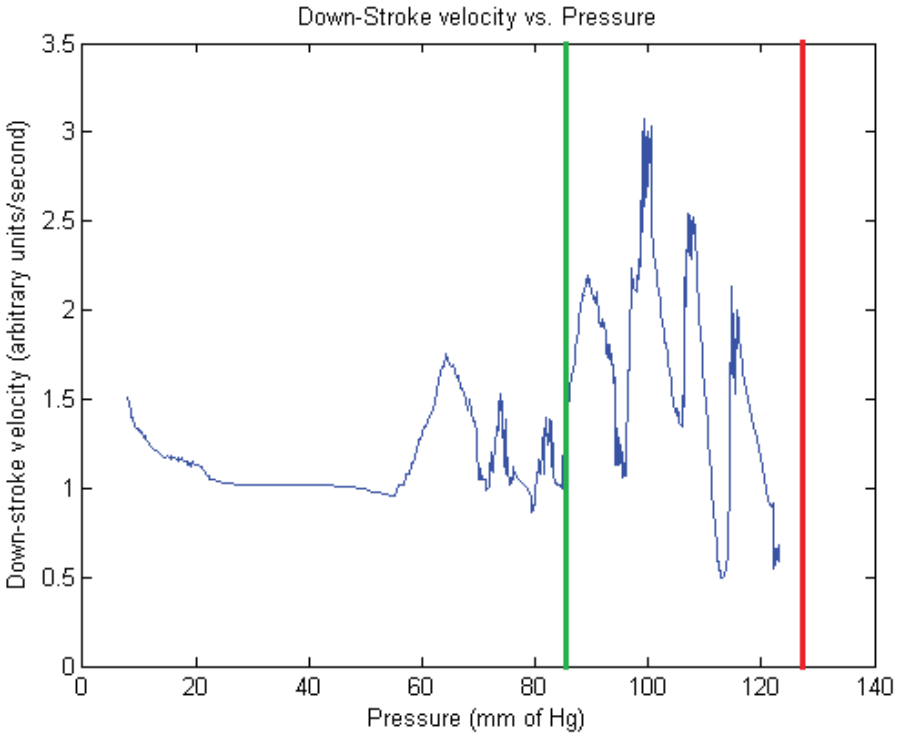

(c)

Figure 5.9. Contd/…

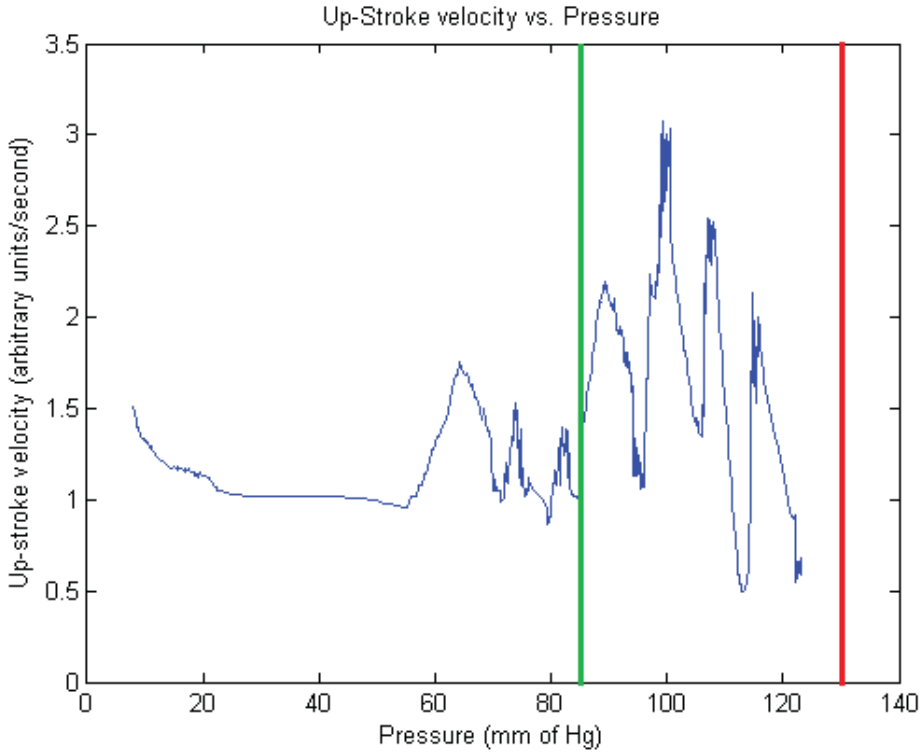

(d)

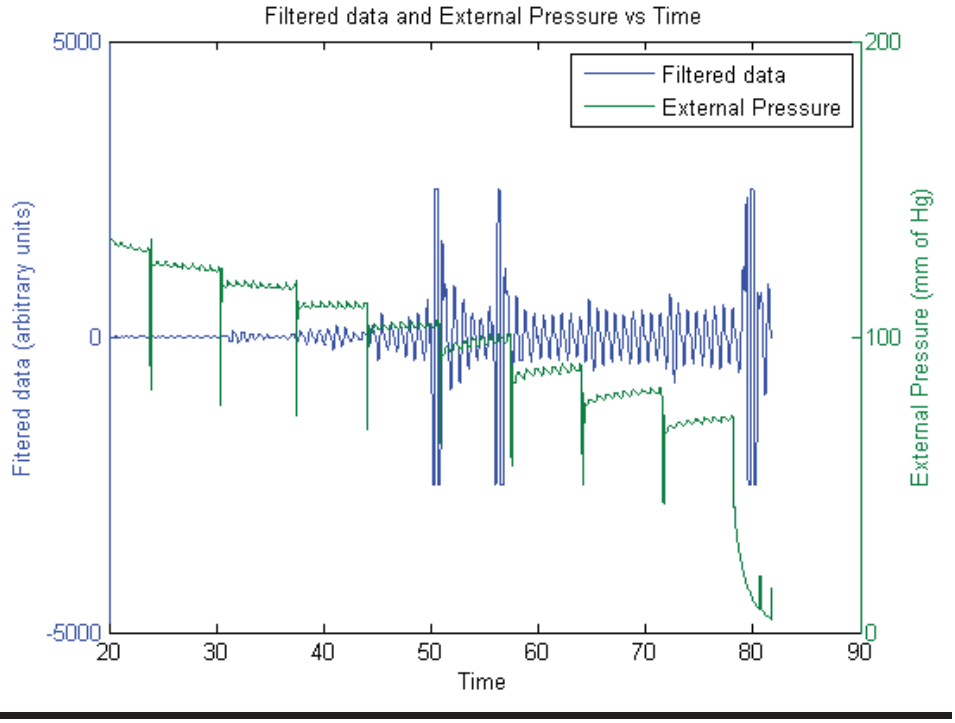

(e)

Figure 5.9. Contd/…

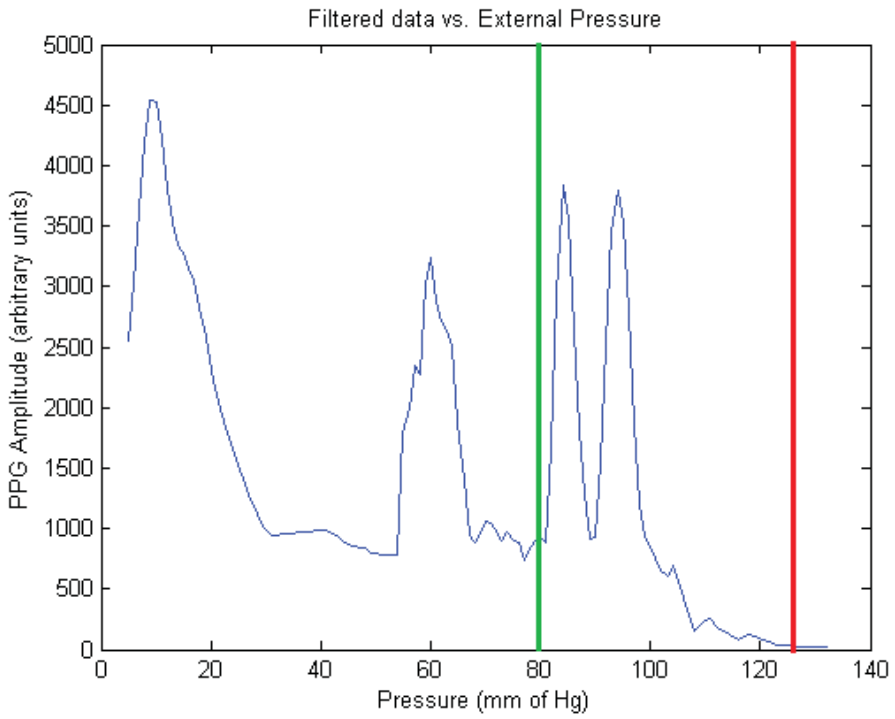

(f)

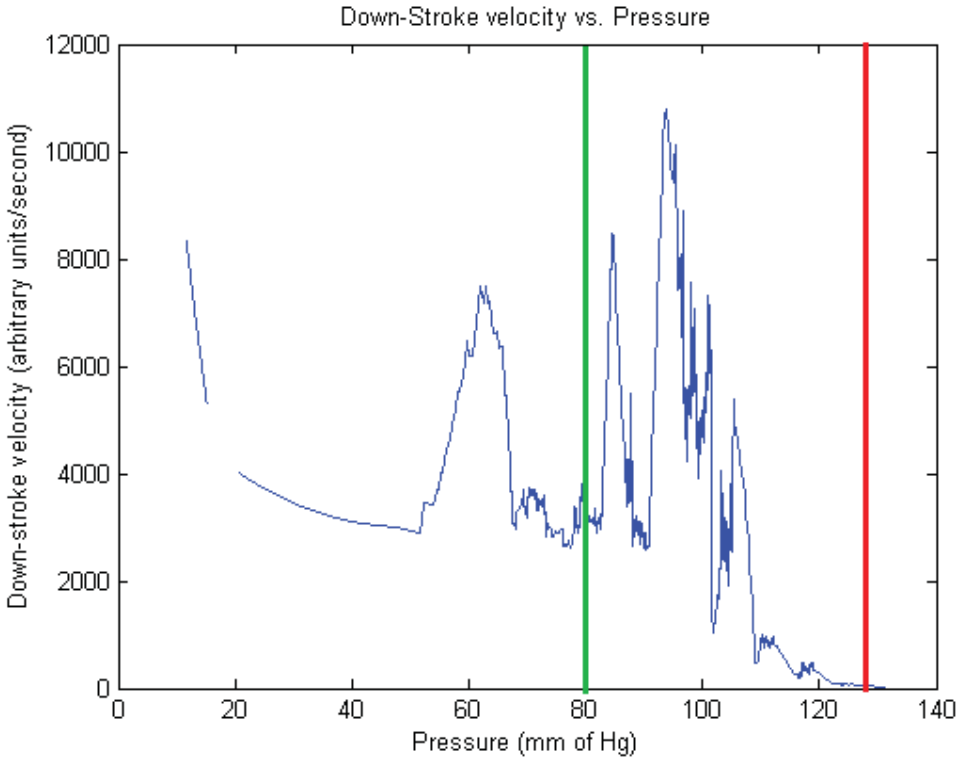

(g)

Figure 5.9. Contd/…

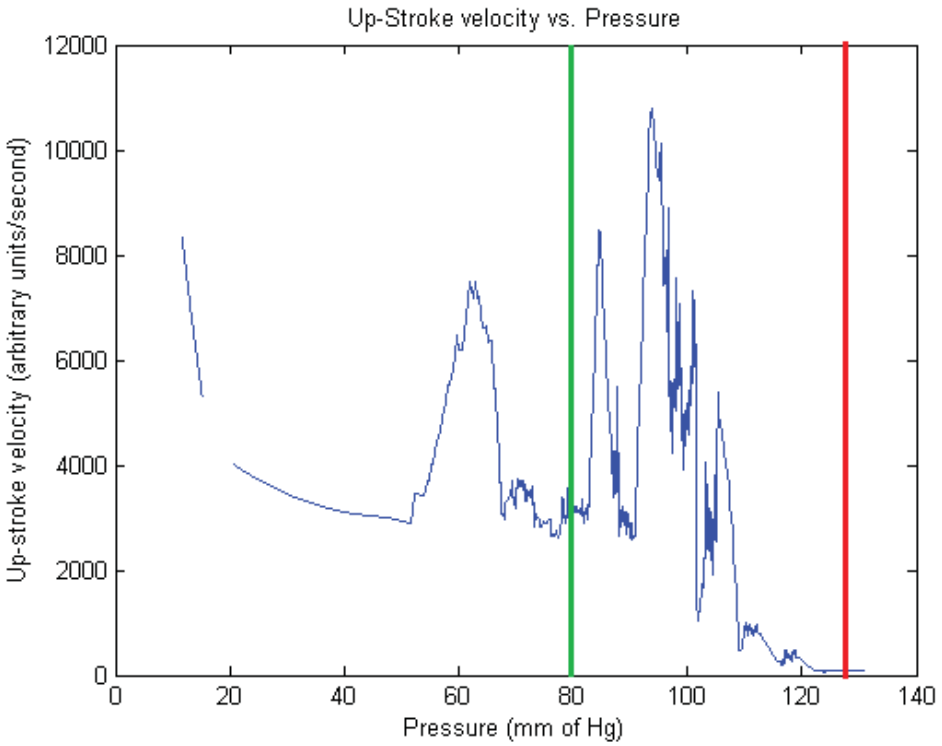

(h)

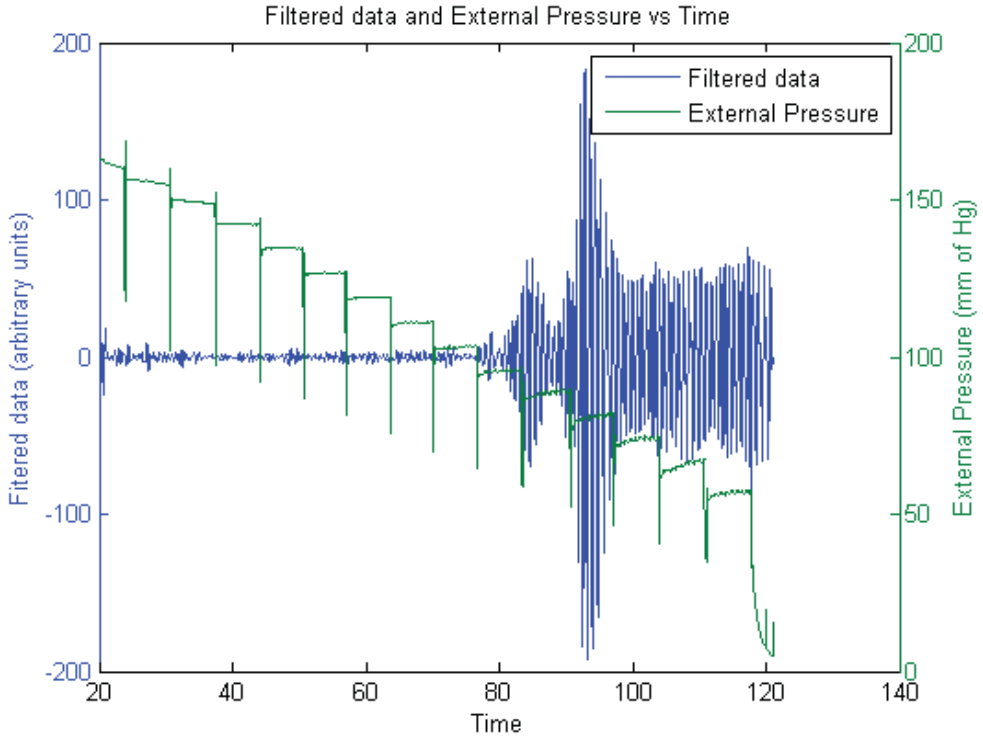

(i)

Figure 5.9. Contd/…

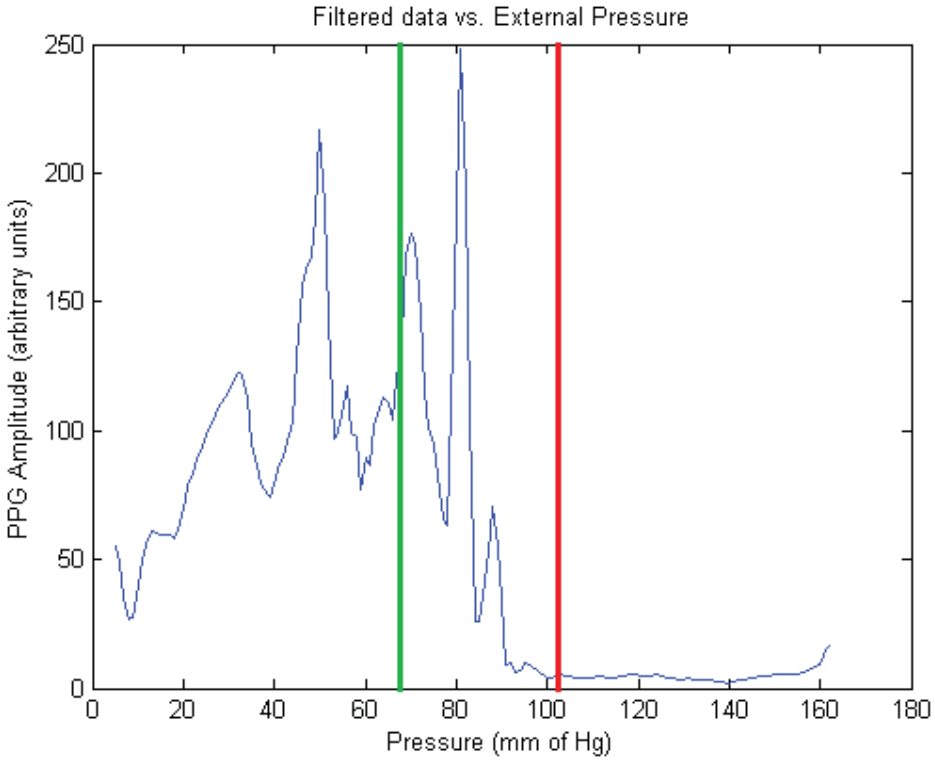

(j)

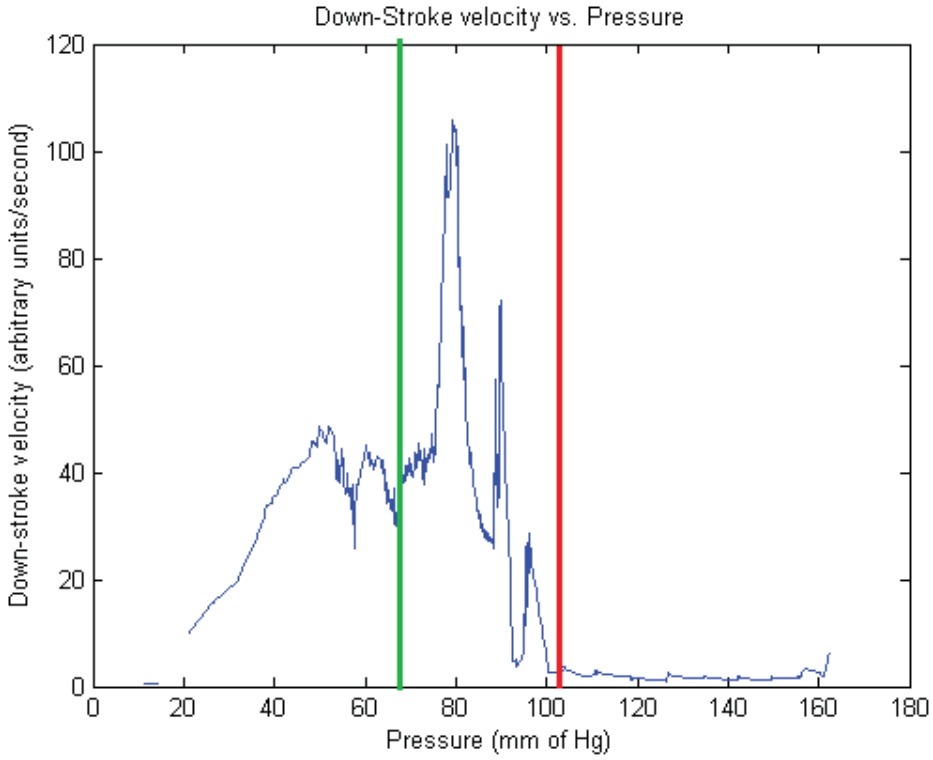

(k)

Figure 5.9. Contd/…

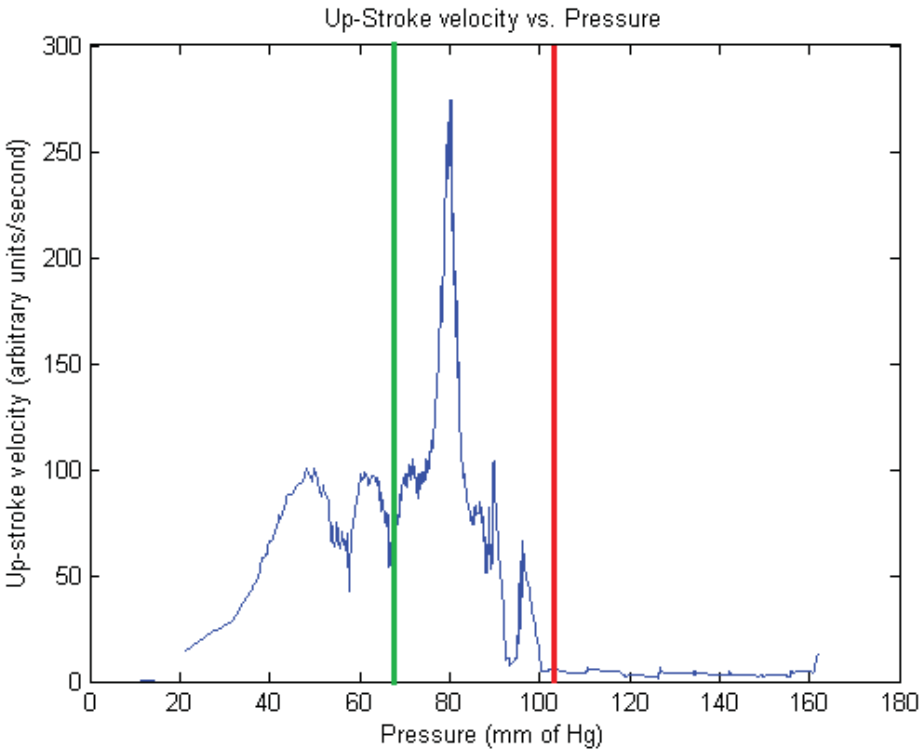

(l)

Figure 5.9. Contd/…

It was noted that even if all subjects didn't show similar PPG-Pressure responses, the data would still be usable to predict pressure if a subject's response was repeatable. For this purpose, two sets of NIBP data was collected from subjects at an interval of 5 minutes. Figure 5.10 shows a sample of the plots obtained.

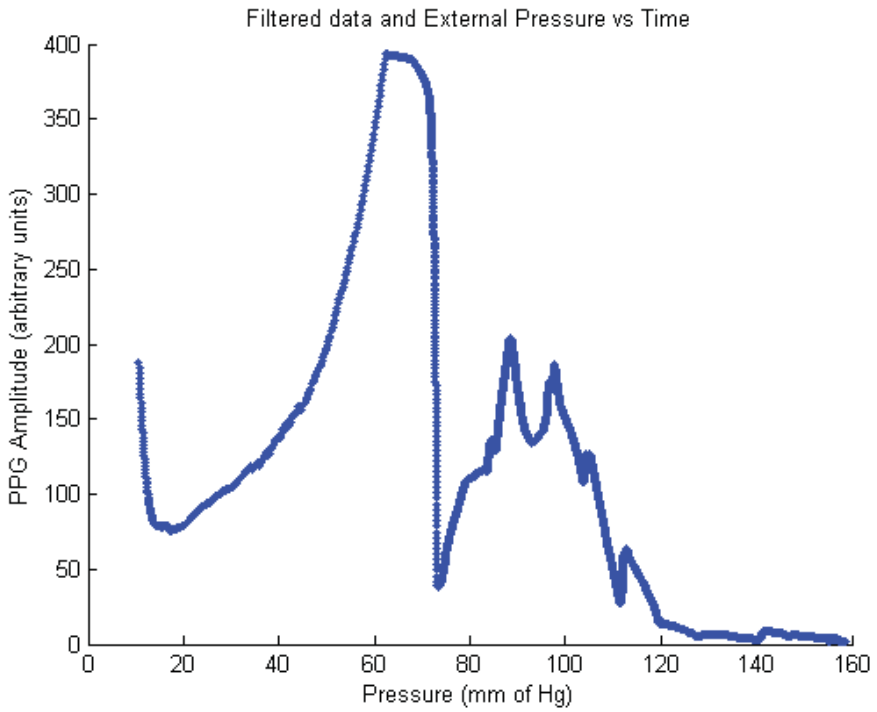

(a)

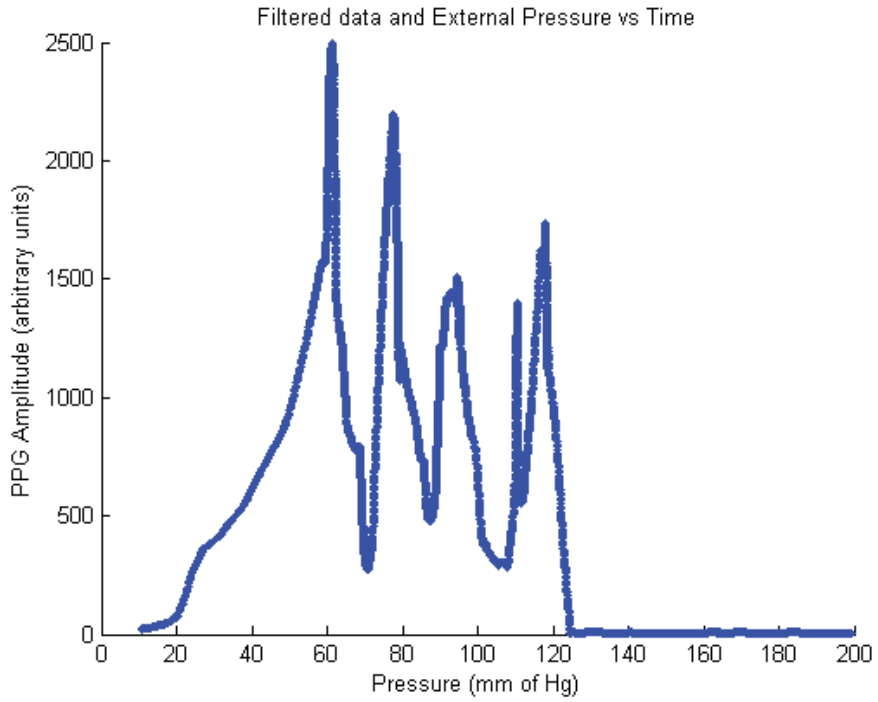

(b)

Figure 5.10. Test of repeatability by recording PPG with external pressure from NIBP device applied at an interval of 5 minutes. (a) shows the initial response and (b) shows the response obtained when the same process was repeated after 5 minutes. Note that the amplitude of the signal itself has gone from ranging around 400 to around 2000.

5.3 Analysis of data collected with no external pressure

Figure 5.11 shows the measured systolic and diastolic pressures of the 20 subjects. The data collected from the 20 subjects was filtered and the amplitudes of the resulting signal was measured. With was no external pressure applied and the subject motionless, the amplitudes still vary by a large amount, as indicated by the high values of standard deviations.

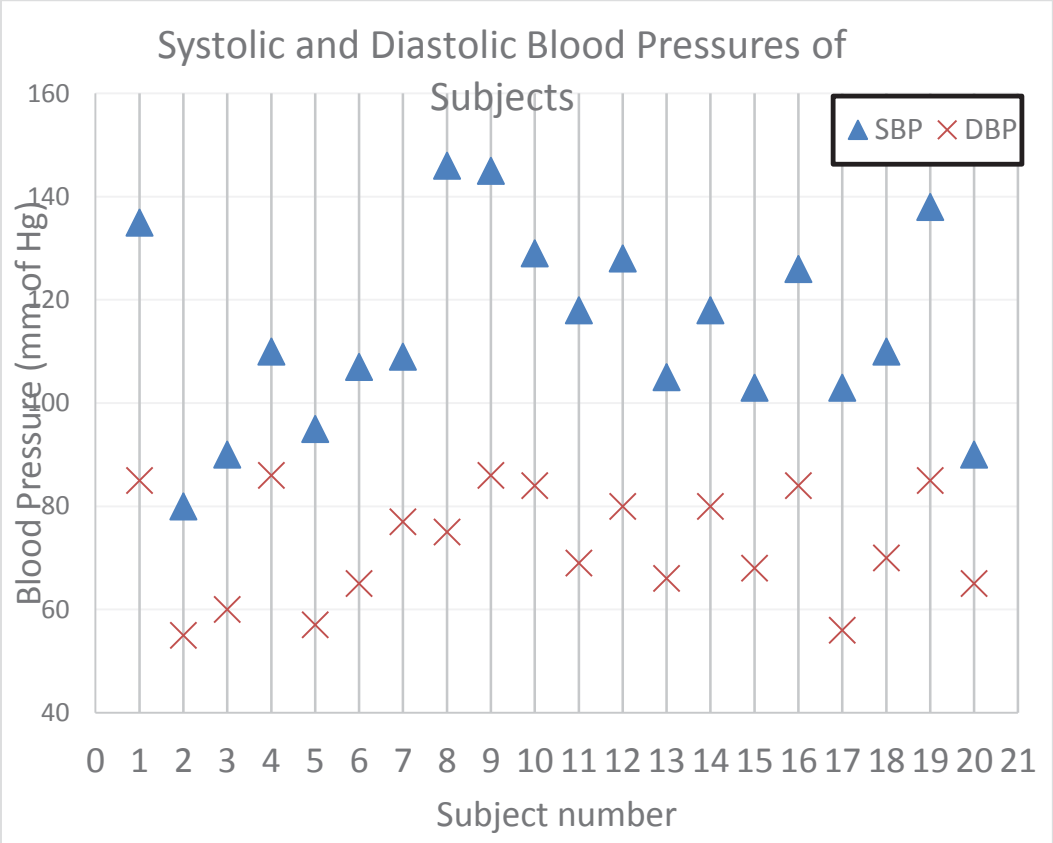

Figure 5.11 Systolic (SBP) and Diastolic Blood Pressures (DBP) of the subjects

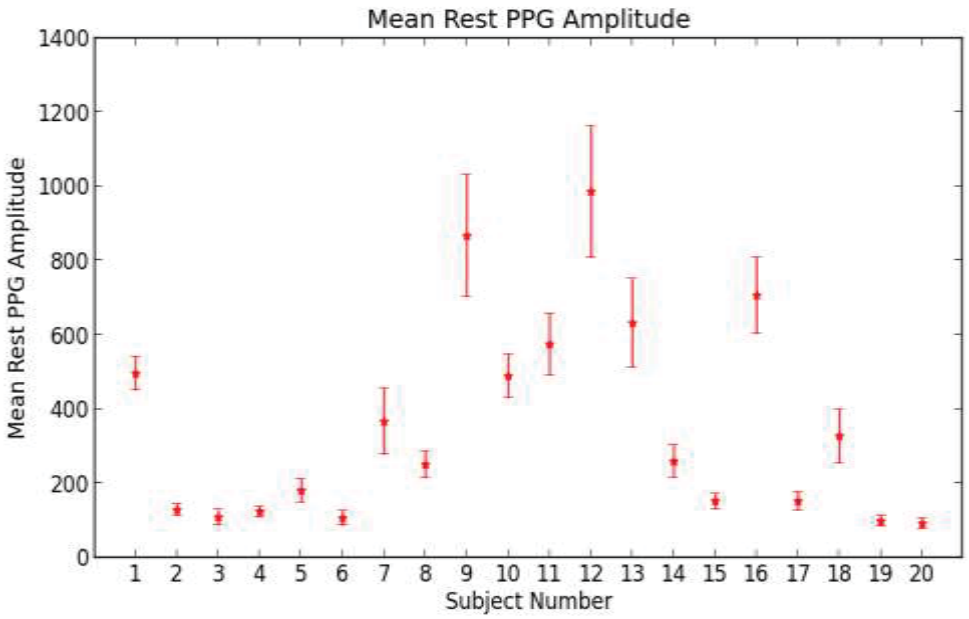

(a)

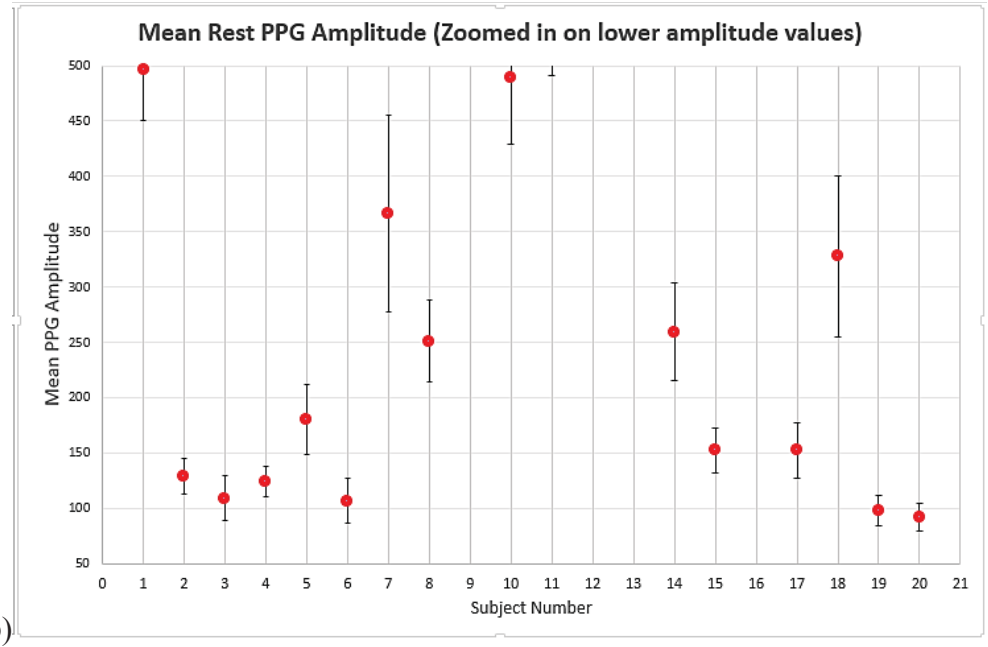

(b)

Figure 5.12 (a). Mean PPG amplitude of 20 subjects at rest along with standard deviations. (b). Modified (a) to show subjects with lower PPG amplitudes.

As described in Section 4.2, the other parameters, viz. up-stroke slope or velocity and down-stroke velocity were also calculated and plotted, as above.

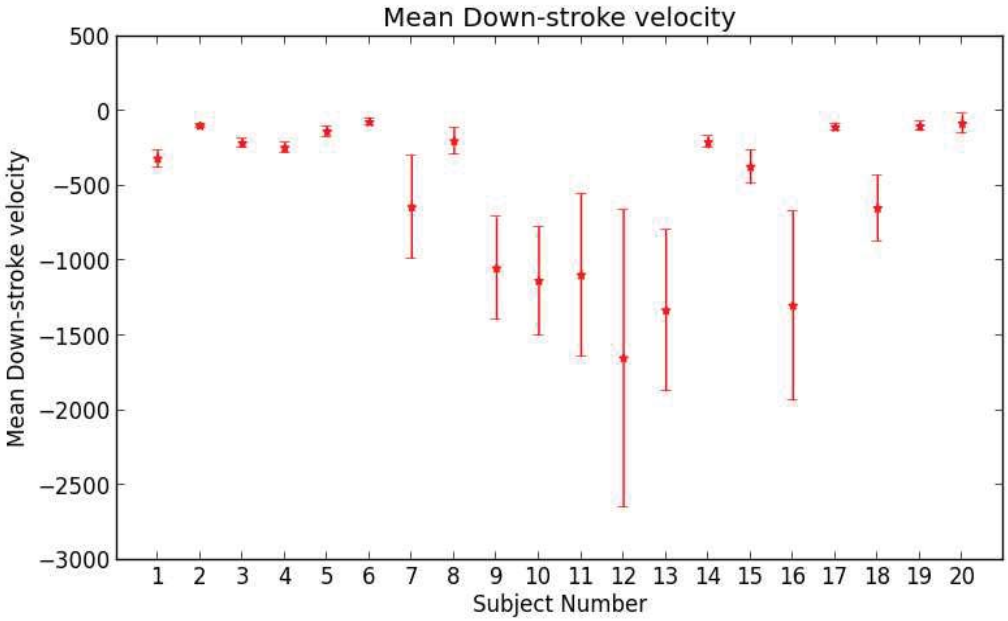

Figure 5.13 Mean Down-stroke velocity or slope of PPG of each subject.

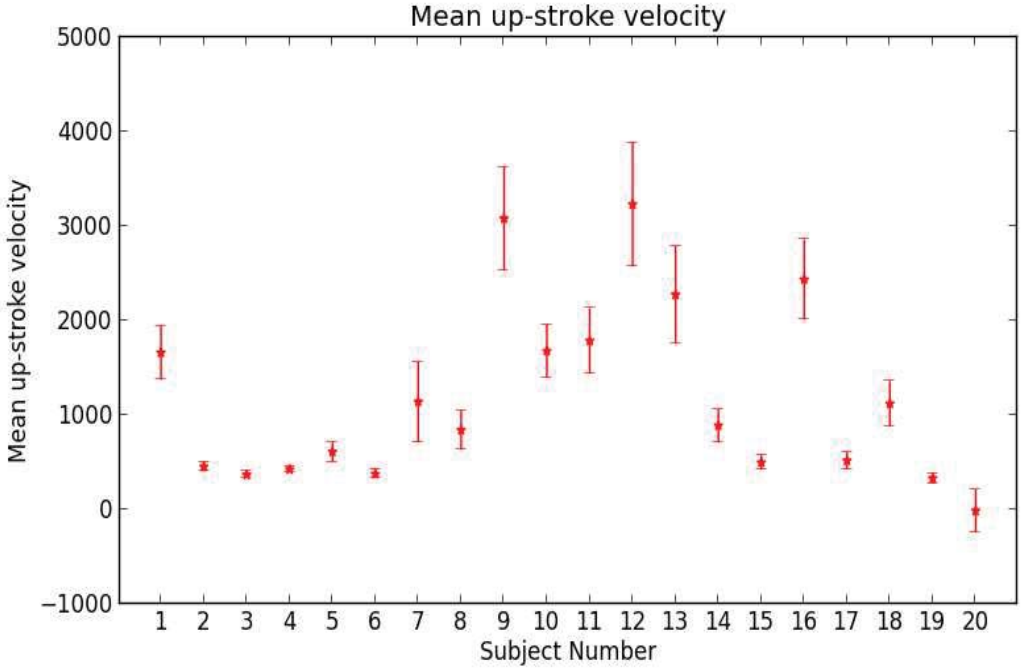

Figure 5.14. Mean Up-Stroke velocity or slope of PPG of each subject

In all these cases, the signal varies too much, as seen from the magnitude of standard deviation, for these parameters of the PPG to be used as a reliable indicator of pressure, especially over long time periods.

In addition to the amplitude and slopes obtained from the PPG, the real-time pressure was computed using equation (6), which was obtained by combining equations (4) and (5). The Young's modulus is of the order of 10^5 to 10^6 Pa. [33] For a vessel in the human finger (of approximately 10^{-2}m diameter and 10^{-3}m wall thickness), the wall volume is of the order of 10^{-6} m^3 per unit length. Since it is difficult to obtain the precise arterial wall volume and the Young's modulus for each subject, non-invasively, the constants were given an arbitrary value of these orders and the real-time pressure was predicted. An example of such a plot is shown in figure 5.15.

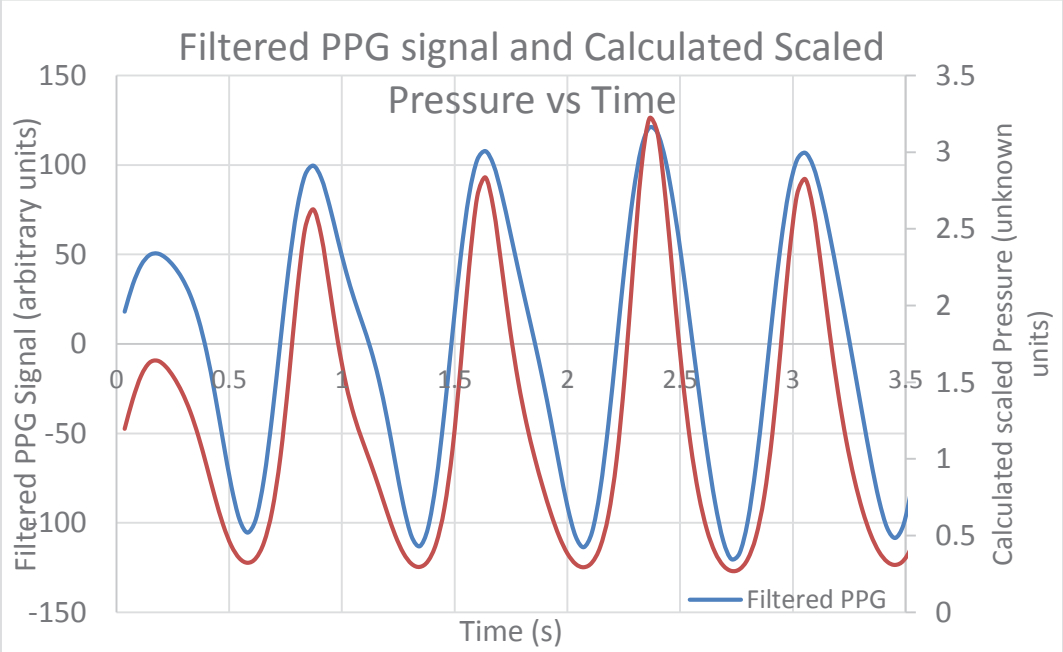

Figure 5.15. Plot of filtered PPG signal and the scaled pressure parameter calculated using (6) vs. time.

The mean amplitude of the calculated scaled pressure was plotted for all the 20 subjects along with the minimum and maximum values of pressure. These plots are shown in Figure 5.16.

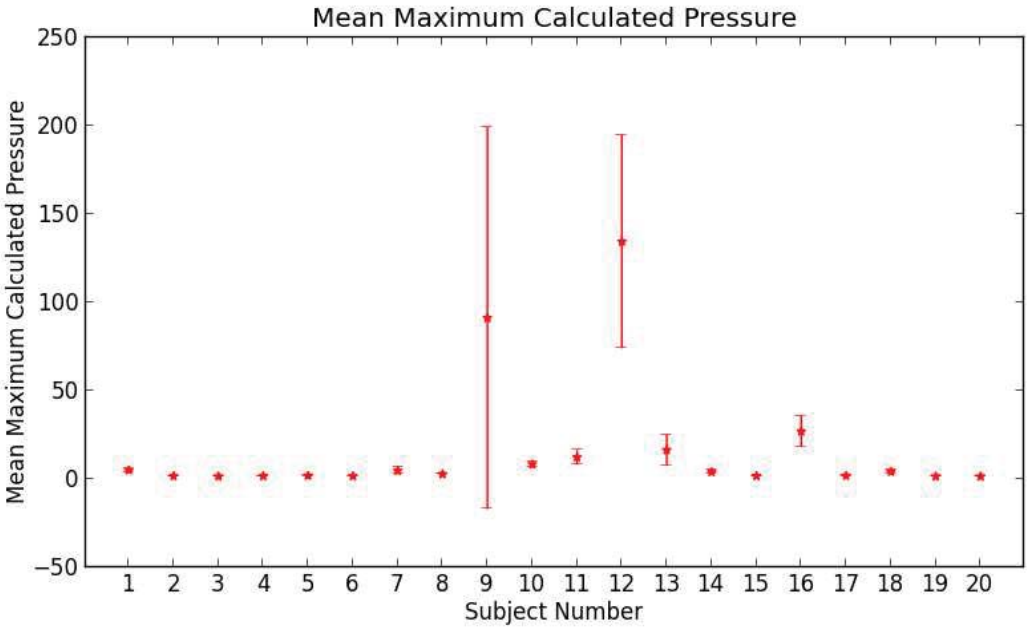

(a)

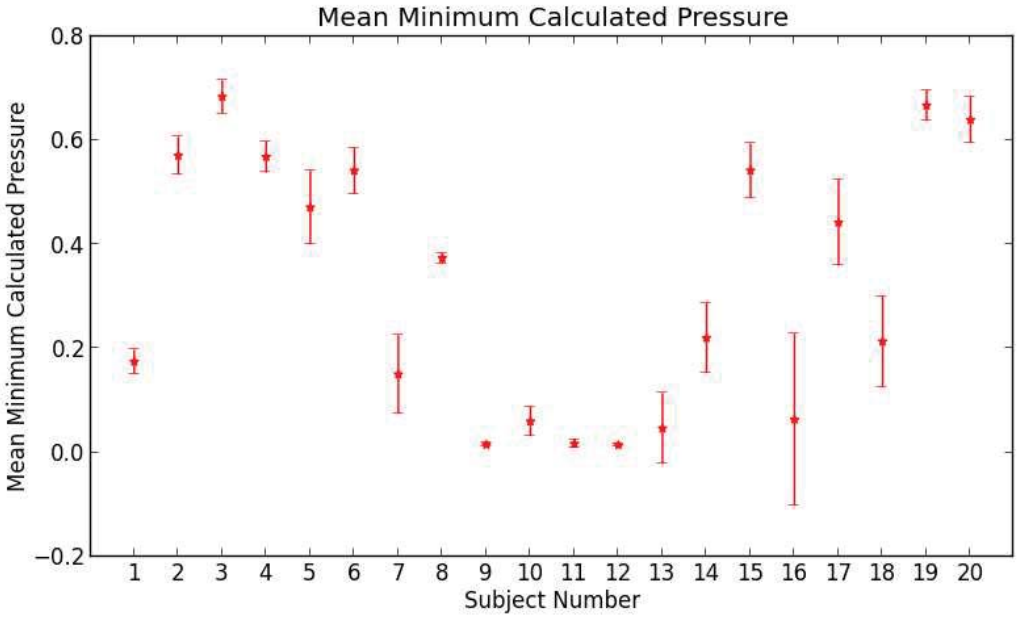

(b)

Figure 5.16. (a) Shows the mean maximum calculated scaled pressure for all the subjects. (b) Shows the Mean Minimum Calculated Scaled Pressure for the subjects and (c) Shows the Mean amplitude, obtained by subtracting the minima from the maxima.

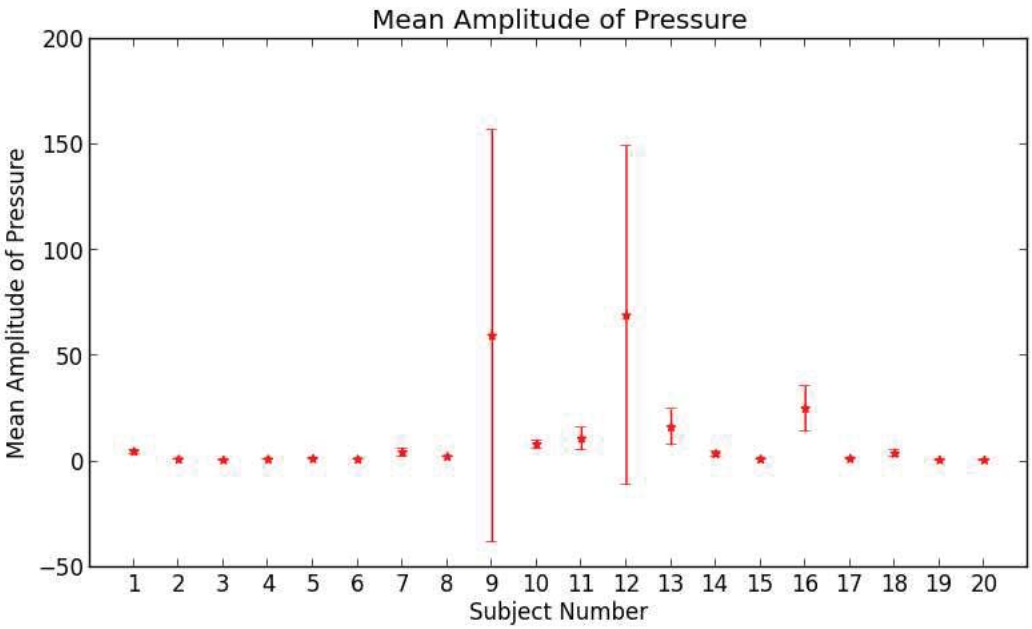

(c)

Figure 5.16. Contd/…

Using the equation obtained in section 4.4, i.e., equation (7) that relates the change in pressure to the intensity of light, the PPG from a subject was scaled up to the measured pressure, which in this case was 145/83. A plot of the scaled pressure vs. time is shown in Figure 5.17. The following chapter discusses the results.

Figure 5.17. Sample scaled-up plot of the calculated pressure using Beer-Lambert Law and Langewouter's relationship

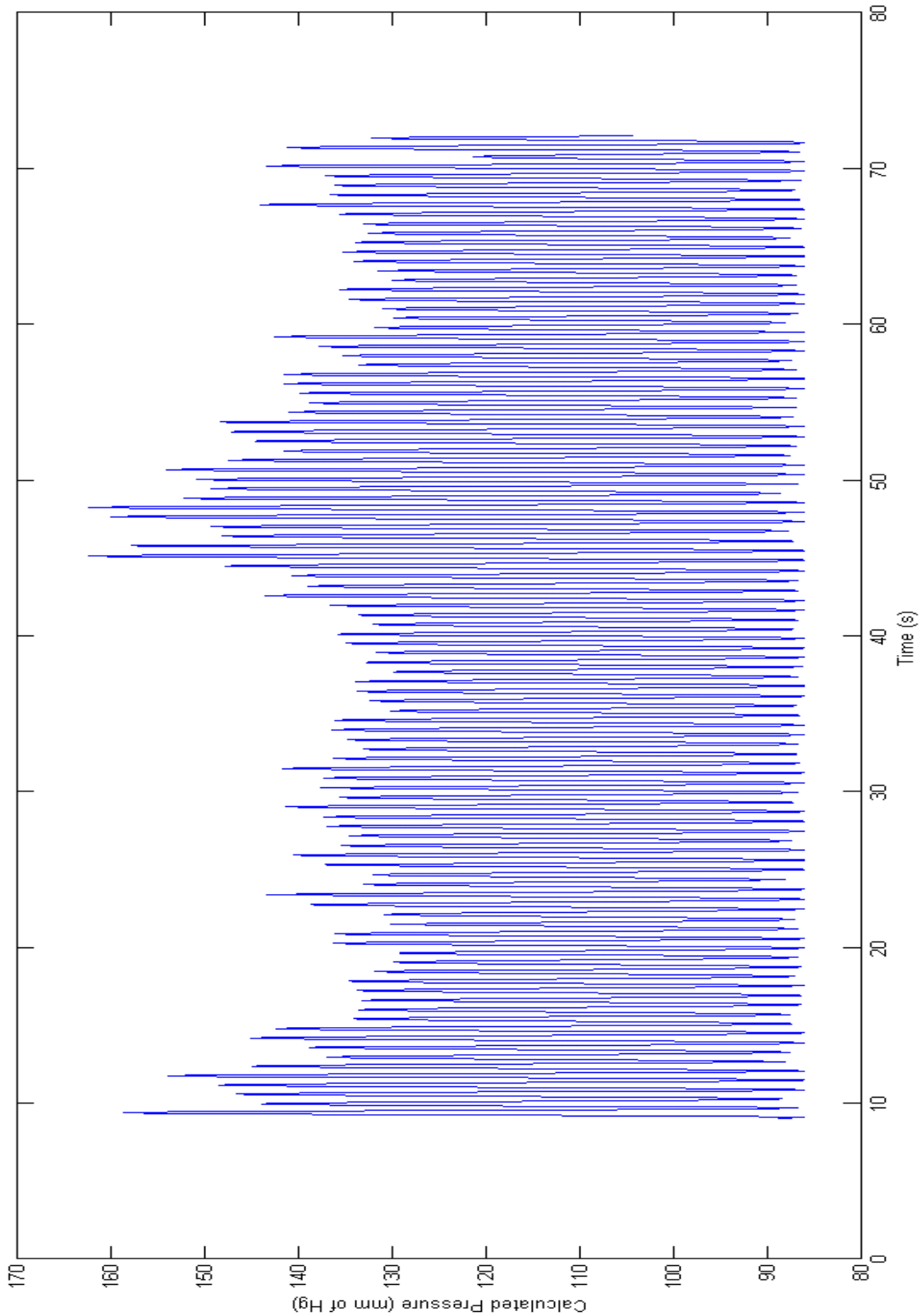
Calculated Pressure (mm of Hg)
170
160
150
140
130
120
110
100
90
80
0
10
20
30
40
50
60
70
80
Time (s)

Chapter 6: Discussion

As the first step in the analysis, three filters were compared and the FIR-IIR filter was determined to perform the best. Analysis of PPG data collected from over 20 subjects, while the NIBP device was in operation, indicated that subjects could be broadly grouped into categories. The PPG data collected when the subjects were at rest indicated that some parameters correlate very well with the blood pressure in certain patients but had larger standard deviations in others.

6.1 Identification of optimal filter

The best filter, for this application, is one which will filter out all frequencies outside the range of interest- which is 0.5Hz to 2 Hz. The Butterworth filter was determined to be unstable, as the filtered signal often saturated, giving erroneous outputs. The performance of averaging filter was better, as the output centered around zero and the signal retained its shape, but taking the average value of the signal over one cycle is not an accurate method of DC removal as the PPG signal is not perfectly symmetric, mainly due to the presence of the venous back-flow peak in the PPG. Moreover, this type of filtering does not account for amplitude changes due to respiration. In comparison, the FIR-IIR filter performs better in terms of stability and DC signal removal in addition to faithful transmission of the alternating component of the PPG waveform. Hence, this filter was chosen for all the experiments.

6.2 Analysis of PPG data collected while NIBP device was in operation

After filtering the PPG data from the subjects, and plotting the amplitude of the PPG signal at different applied external pressures, as shown in Figure 5.9, it was observed that all the subjects shared a common feature- the swift increase in amplitude of the PPG signal when the systolic pressure was reached. At this point, blood that was held back by the occlusion in the artery, introduced by the cuff, rushes forward. As the diastolic pressure is approached, there is no common pattern that can be observed in all subjects. While in all subjects, there is a general decrease in amplitude around the diastolic pressure, compared to the amplitude at nearby values of pressure, in some cases the diastolic point is marked by a minimum, whereas in others it lies on a few mm of Hg above the minimum. In very few subjects - 2 out of the 20, the diastolic pressure was reached at a point of a local maximum. However, it should be noted that this local maxima was lower in amplitude than the other peaks or maxima in the amplitude - pressure curve. Once the diastolic pressure has been reached, the signal becomes more unpredictable. It was expected that the amplitude of the filtered PPG signal would remain steady. However, only one out of the 20 subjects showed this pattern. In many others, the signal decreased in amplitude, after the diastolic pressure and in rare cases – 2 out of the 20 subjects studied, the amplitude increased. Table 2 in the Appendix summarizes the patterns observed.

Based on these observations and accounting for common factors seen, the collected data was broadly classified into three types, as described below and depicted

in Figure 5.9. It should be noted that Figure 5.9 is only one representative sample of the pressure-PPG response curve from each of the categories.

1. Steady increase in amplitude beyond systolic pressure, a sharp decrease at the diastolic pressure and a decrease in amplitude, which settles at a relatively stable value as the external pressure approaches zero.
2. Steady increase in amplitude beyond systolic pressure, a sharp decrease at the diastolic pressure and an increase as the external pressure approaches zero.
3. Steady increase in amplitude beyond systolic pressure, followed by a decrease in amplitude approximately 5-10mm of Hg above diastole. Further decrease in pressure makes the signal settle at a value, albeit a little unevenly.

Although there seems to be an obvious correlation between the increasing pressure and the decreasing amplitude, and the systolic point can be identified as the time when the PPG signal reappears, it is not easy to identify the point where the diastolic pressure is reached. The anomalous behavior at the point where the diastolic pressure occurs could be due to change in the arterial wall compliance, which affects the constants used in equation (3). This change in external pressure also affects the flow rate of blood within the brachial artery, making the flow turbulent and thereby affecting the volume of blood reaching the finger probe. The degree of turbulence introduced varies with the subject's physiology.

Granting that the amplitude of the PPG signal changes drastically with change in pressure, the up-stroke and down-stroke slopes seem more consistent with the pressure change. The slope vs. time plots in Figure 5.9 indicate that the up-stroke and

down-stroke velocities or slopes are more consistent with change in pressure. From the slope vs. pressure plots in Figure 5.9, it can be seen that both systole and diastole represent local minima, i.e., there is a sharp increase in slope at those two points. However, it is easier to identify systole as the point before which the slope was negligible, whereas there are many other minima in the slope-pressure profile, which make accurate prediction of diastole difficult. In most cases, the other local minima were at higher values than the slope at diastole. Nevertheless, the slopes or velocities roughly followed the trend set by the amplitude. The velocities reflect the similar patterns as that of the amplitude because the denominator in the formula used to compute the slope or velocity is time and this time is determined by the heart rate. During the course of the experiment, the subject is seated and in such conditions the heart rate does not change by large amounts.

6.3 Analysis of PPG data obtained with no external pressure

From the previous observations, it was noted that the up-stroke and down-stroke velocities make for better indicators of systolic and diastolic pressures. As the aim of this project is to be able to identify a parameter that can be used independently (without an external cuff) to determine blood pressure, data collected from patients at rest, without the cuff or with no external pressure was analyzed to verify if the parameters in the PPG signal, inspected previously remain fairly constant over a period of 1 minute. As in the case with application of external pressure, the amplitude showed higher variability than the up and down-stroke velocities. However, the amplitude and the up-stroke velocity showed a standard deviation of between 10 and 20% from their mean value. The variability in the down-stroke velocity was higher- going up to 40% of the mean value in some subjects. This can be explained by the intervention of the venous

back-flow pulse, which introduces an unpredictability in the time taken for the PPG signal to reach its minimum.

6.5 Analysis of Computed Pressure

The continuous, real-time pressure obtained from the above equation is notably a more consistent indicator of pressure, with standard deviations as low as 4% of the mean value, when data is collected over a period of approximately 30-40s. However, over longer time durations (more than 1 minute), this signal also becomes highly variable, increasing the standard deviation, in some cases, to over 100%. Although it seems as though the minimum value of the calculated pressure is fairly stable, similar to the diastolic pressure, and has a lower standard deviation from the mean, in approximately 50% of the subjects, the standard deviation lies anywhere between 30 and 60%.

As can be seen in Figure 5.16, some subjects exhibited very large deviations in the calculated pressure. This is unrealistic as the subject was at rest and unperturbed when the data was taken. Although the standard deviations in 5.15(b) are significantly lesser than the others, this minimum pressure value represents the diastolic value, which does not change much in real life. When a patient is coding, their DBP remains fairly constant while systolic blood pressure (SBP) undergoes drastic changes. So, it was theorized that minima on the calculated pressure curve could represent the diastolic pressure (as it does not vary with change in PPG amplitude, as shown in Figure 5.14). In addition, the variability in the maxima and minima highlight the variability in the net amplitude of the scaled signal. The standard deviations in most of the subjects was higher than 10% of the mean. For a patient with a systolic blood pressure of 130mm of

Hg, a 10% variation can imply that the patient's actual blood pressure is anywhere between 117 mm of Hg, which is healthy and normal, or 143mm of Hg, which is high and unhealthy.

However, it must be remembered that the pressure-volume relationship used to compute the real-time pressure in equation (6) discussed in chapter 4 was calculated for the aorta and larger blood vessels like the carotid artery. At an extremity of the body, like the tip of a finger, this relationship is highly influenced by many parameters, including the length of the blood vessel from the heart to the finger. As illustrated by Figure 6.1, [34], [35] the shape of the PPG in itself varies depending upon the location. More importantly, the effect of venous back-flow becomes more prominent when moved further away from the heart. [36] This second peak adds an excess pressure to the arterial wall pressure we calculate using equation (6) – the relationship that describes change in arterial pressure with change in diameter of the artery. As can be seen in Figure 6.1, a better estimate of the arterial blood pressure may be obtained using (6) if the PPG data is collected from the subject's fore-arm, over A. brachialis. It will also be helpful to compensate the PPG device for movement-induced artifacts, as that is one of the primary factors leading to an erroneous signal.

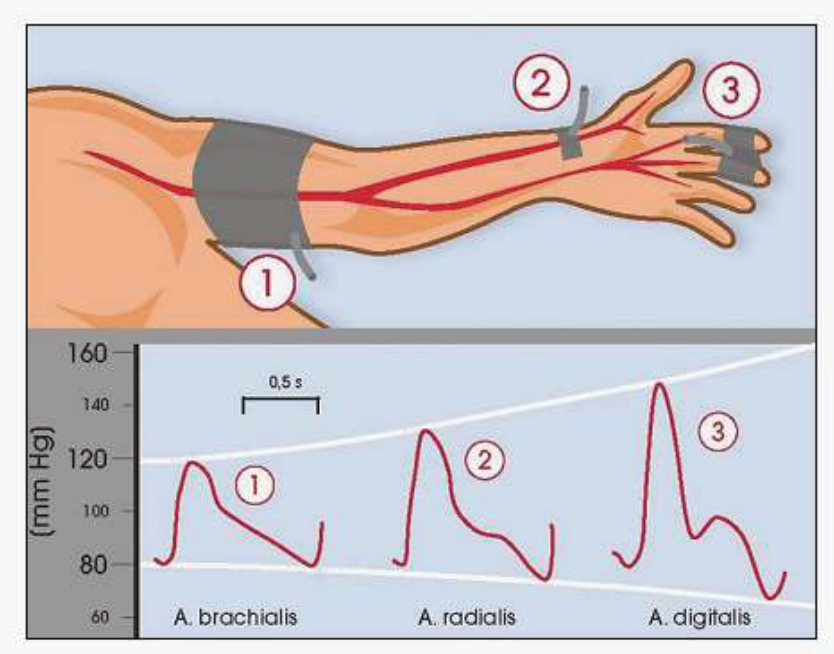

Figure 6.1. PPG measured at three locations- 1. Over the brachial artery in the forearm (A. brachialis), 2. Over the radial artery near the subject's wrist (A. radialis) and 3. Over a finger or digit (A. digitalis). [34]

The different parameters analyzed during this project exhibit a large degree of variability between subjects. Yet, in most subjects, the real-time pressure calculated when the subject was at rest was relatively a better indicator of the actual pressure change compared to the other parameters. The amplitude and up and down-stroke slopes of the PPG varies with a fairly high standard deviation. This could, however, be attributed to the influence of respiration on the blood volume. While an attempt was made to remove the effect of the breathing cycle from the PPG by filtering the signal, a better method could be devised to account for the wide variability in the respiratory rates of different subjects.

6.4 Conclusion and Future Scope

Even though, the PPG alone does not appear to be a sufficiently informative signal that can inform us the blood pressure, it is possible to improve the accuracy of this signal by measuring the PPG at a point closer to the heart- for example, the brachial artery. While the data from all the subjects did not show a single common pattern that was repeatable with a fair degree of accuracy, a majority of the subjects demonstrated a decrease in PPG amplitude when the external pressure applied was equal to the diastolic pressure and the slope of the PPG showed a minimum both at systole and diastole. It is possible that with better methods of measuring the PPG, an improved correlation might be observed.

Another possible improvement that can be made to the PPG signal is to suppress the effect of venous back-flow. As seen in figure 5.2, the Fast Fourier Transform of the PPG data shows a spread over a frequency range of approximately 1Hz. This variability is primarily due to the change in time taken for the arterial signal to reach its minimum because the venous signal introduces a peak of its own in the PPG. It is difficult to filter this venous back-flow pulse because it has the same frequency as that of the arterial pulsations. It must be noted from figure 6.1 that the venous back-flow is almost negligible in the PPG signal obtained from the brachial artery. Such measurement is a possible solution to the highly variable signal obtained from a finger oximeter. In addition, collecting PPG data and intra-arterial pressure data from subjects prone to higher variability in blood pressure, simultaneously will greatly aid in the identification of any characteristics in the PPG signal that change with the intra-arterial pressure measured.

In the future, if a parameter can be identified that is consistent with measured average blood pressure data over fairly long intervals of time - say 5 minutes, the real-time accuracy of the method could be evaluated, by comparing the technique developed with measurements made from an intra-arterial line. The robustness of the device could be determined, and the device could be made less sensitive to motion artifacts, so as to be used in tilt-table tests. Including an accelerometer to sense motion in the finger oximeter can help compensate for the artifacts introduced in the PPG signal due to movement, especially during clinical procedures like tilt-table tests. The accelerometer will be able to sense the height at which the limb is and the device can be programmed to compensate for the change in amplitude with respect to posture. Hence, despite the PPG signal being quite variable and dependent on many parameters, part of a complex system, with a few improvements to the device's sensitivity, the arterial blood pressure can be monitored continuously and non-invasively.

APPENDIX

Table 1. Subjects' systolic and Diastolic blood pressure data.

Subject Number	Systolic Blood Pressure (mm of Hg)	Diastolic Blood Pressure (mm of Hg)
1	110	70
2	85	56
3	120	85
4	90	60
5	110	75

Table 2. Patterns observed when PPG data was collected with NIBP device in operation.

Parameter	**External Pressure stage**	**Observations**
Amplitude of filtered PPG signal	Systole	Sharp increase in amplitude
	Diastole	1. Local minimum, or a decrease in amplitude between systole diastole followed by an increase between diastole and zero 2. Between 5-10mm of Hg above a local minimum
	Between Diastole and zero	1. Increase 2. Decrease 3. Stable
Up-Slope and Down-slope of the filtered PPG signal	Systole	Rapid increase in slope
	Diastole	Local minimum, but difficult to discern from other minima.
	Between Diastole and zero	Follows similar trend as amplitude

Table 3: Data Collected when patient was at rest, with zero external pressure

Subject No.	SBP	DBP	MAP	Range	Mean Rest PPG Amplitude	Std Dev (Rest PPG Amp)	Mean down-stroke velocity	Std Dev	Mean up-Stroke velocity	Std Dev	Mean Max. Pr	Std Dev	Mean Min. Pr	Std Dev	Mean Pr Ampl	Std dev Pr Ampl
1	135	85	110	50	496.2	45.8	-318.78	59.48	1656.35	284.77	4.905304	0.895378	0.174673	0.022867	4.730631	0.916249
2	80	55	67.5	25	128.7427	15.73352	-100.433	9.911284	451.033	46.36275	1.626543	0.073213	0.570007	0.036353	1.056931	0.103938
3	90	60	75	30	108.9033	20.22989	-215.336	28.91004	365.284	35.69996	1.423997	0.059306	0.682953	0.031794	0.742464	0.08814
4	110	86	98	24	124.2439	14.07945	-245.52	31.37346	422.0581	27.54668	1.611772	0.065257	0.567722	0.029873	1.052177	0.074786
5	95	57	76	38	180.6634	31.58652	-137.592	35.53077	607.7117	104.646	1.82339	0.166729	0.470722	0.070325	1.352668	0.231424
6	107	65	86	42	106.6872	19.98751	-75.0998	19.28876	373.014	42.65159	1.585504	0.064471	0.541248	0.043894	1.044256	0.102111
7	109	77	93	32	366.5696	88.76612	-641.995	343.8621	1137.878	425.5733	4.615397	1.881621	0.15016	0.075627	4.465237	1.936076
8	146	75	110.5	71	250.7693	36.98779	-201.413	88.94798	838.1692	209.03	2.702001	0.087417	0.373236	0.010222	2.328765	0.094389
9	145	86	115.5	59	866.6024	164.1353	-1051.06	341.9661	3075.209	545.1619	90.96457	108.0324	0.01504	0.003955	59.5254	97.4192
10	129	84	106.5	45	489.2689	59.75033	-1135.06	363.1466	1674.651	279.0756	8.285639	1.8143	0.059626	0.02791	8.226768	1.832392
11	118	69	93.5	49	574.8969	83.58054	-1095.84	543.6649	1781.33	345.4315	12.23065	4.07732	0.017028	0.008253	10.91249	5.419078
12	128	80	104	48	985.525	177.6956	-1650.85	992.0228	3223.658	655.2868	134.2049	60.33404	0.014333	0.001701	69.12154	80.0992
13	105	66	85.5	39	632.0312	119.3973	-1332.04	539.6954	2270.71	512.4854	16.33342	8.539134	0.046348	0.06795	16.29054	8.560817
14	118	80	99	38	259.3082	44.14612	-208.929	41.04429	885.8787	173.1558	3.904438	1.06642	0.21987	0.067151	3.684568	1.126365
15	103	68	85.5	35	152.5013	20.23187	-373.589	114.0254	495.5733	76.65295	1.696137	0.122281	0.541393	0.052135	1.160052	0.170765
16	126	84	105	42	706.13	103.9036	-1300.19	632.4329	2430.798	422.2963	26.82752	8.764309	0.164733	0.06342	25.15445	10.64959
17	103	56	79.5	47	152.2889	25.31749	-109.572	20.61932	515.0691	89.55891	1.832793	0.200117	0.441508	0.082466	1.396302	0.260078
18	110	70	90	40	327.7732	72.46365	-649.408	220.0051	1116.708	238.7766	4.050575	1.27022	0.213109	0.087508	3.837466	1.344637
19	138	85	111.5	53	98.36794	13.72175	-101.879	29.61906	329.1526	53.17146	1.459163	0.054557	0.666227	0.029678	0.771478	0.197869
20	90	65	77.5	25	92.24103	12.82189	-84.5431	65.71755	226.8712	16.109	1.412567	0.055037	0.638725	0.043952	0.718807	0.278552

REFERENCES

[1] R. S. Vasan, M. G. Larson, E. P. Leip, J. C. Evans, C. J. O'Donnell, W. B. Kannel and D. Levy, "Impact of high-normal blood pressure on the risk of cardiovascular disease," *New England Journal of Medicine,* vol. 345, no. 18, pp. 1291-1297, 2001.

[2] Mayo Clinic Staff, "Low blood pressure (Hypotension)," Mayo Clinic, 19 5 2011. [Online]. Available: http://www.mayoclinic.com/health/low-blood-pressure/DS00590/DSECTION=causes.

[3] Mayo Clinic Staff, "High blood pressure (hypertension)," Mayo Clinic, 21 1 2011. [Online]. Available: http://www.mayoclinic.com/health/high-blood-pressure/HI00062.

[4] [Online]. Available: http://store.gomed-tech.com/nellcor-oximax-spo2-finger-sensor-reusable-p1536.aspx.

[5] O. Abdallah and A. Bolz, "Chapter 7: Adaptive Filtering by Non-Invasive Vital Signals Monitoring and Diseases Diagnosis," in *Adaptive Filtering Applications*, 2011.

[6] D. r. o. w. o. DestinyQx and R. a. S. b. xavax, "Wiggers Diagram," Wikimedia Commons, 20 March 2012. [Online]. Available: http://en.wikipedia.org/wiki/File:Wiggers_Diagram.svg. [Accessed 30 05 2013].

[7] K. Shelley and S. Linder, "Venous Pulsation and PPG," [Online]. Available: http://en.wikipedia.org/wiki/File:VenousPulsationAnd_PGG.png.

[8] L. Cromwell, F. Weibell and E. Pfeiffer, Biomedical Instrumentation and Measurements, Prentice Hall, 1980.

[9] W. Nguyen and R. Horjus, "Heart Rate Monitoring Control System Using Photoplethysmography," San Luis Obispo, 2011.

[10] A. Beckett and J. B. Stenlake, Practical Pharmaceutical Chemistry: Part II Fourth Edition (Vol. 2). Continuum., 1988.

[11] M. Hayes, "A new method for pulse oximetry possessing inherent insensitivity to artifact," *IEEE Transactions on Biomedical Engineering,* April 2001.

[12] S. Eckert, "100 Jahre Blutdruckmessung nach Riva-Rocci und Korotkoff: Rückblick und Ausblick," *Journal für Hypertonie,* vol. 10, no. 3, p. 7, 2006.

[13] J. Hérisson, The Sphygmomanometer, an instrument which renders the action of arteries apparent to the eye with improvement of the instrument and prefatory remarks by the translator, London: Longman, 1835.

[14] M. Gavaghan, "Vascular Hemodynamics," *AORN Journal,* 01 08 1998.

[15] V. K, Die Lehre vom Arterienpuls in gesunden und kranken Zuständen gegründet auf eine neue Methode der bildlichen Darstellung des menschlichen Pulses, Braunschweig: Vieweg und Sohn, 1855.

[16] M. EJ, "Recherches sur l'état de la circulation d'après les caractères du pouls fourmis par le noveau sphygmopraphe," *J Physiol homme anim,* 1869.

[17] R. R. S and 1896, "Un sfigmomanometro nuovo.," *Gaz Med Torino,* vol. 47, pp. 981-996, 1896.

[18] K. NS, "K voprosu o metodoach eesldovania krovyanovo davlenia," *Imperatoor Vorenno JzV Med Akad,* 1905.

[19] N. Korotkov, "A contribution to the problem of methods for the determination of the blood pressure," *Izvestiya Imperiatorskoi Voenno-Meditsinskoy Akademii 11,* pp. 365-367, 1905.

[20] J. Peňáz, "Photoelectric Measurement of blood pressure, volume and flow in the finger," in *Digest of the 10th international conference on medical and biological engineering*, Dresden, 1973.

[21] R. Grüllenberger and J. Fortin, "DEVICE FOR CONTINUOUS, NON-INVASIVE MEASUREMENT OF ARTERIAL BLOOD PRESSURE AND USES THEREOF". Munich, Germany: Patent European Patent No. EP 2101633, 20 July 2011.

[22] M. Nelson, M. Cevette, M. Covalciuc, R. T. Hurst and A. J. Tajik, "Noninvasive measurement of central vascular pressures with arterial tonometry: clinical revival of the pulse pressure waveform?," in *In Mayo Clinic Proceedings, Elseiver*, 2010.

[23] D. A. Colquhoun, K. Forkin, D. Bogdonoff, M. Durieux and R. Thiele, "Non-invasive, minute-to-minute estimates of systemic arterial pressure and pulse pressure variation using radial artery tonometry," *Journal of Medical Engineering and Technology,* vol. 37, no. 3, pp. 197-202, 2013.

[24] S. PA*, A. Reisner and H. Asada, "Wearable, Cuff-less PPG-Based Blood Pressure Monitor with Novel Height Sensor," in *IEEE EMBS Annual International Conference*, 2006.

[25] C. Norris, A. Beyrau and R. Barnes, "Quantitative Photoplethysmography in chronic venous insufficiency: A new method of non-invasive estimation of ambulatory venous pressure," *Surgery,* 1983.

[26] G. Gorsuch and R. Kempsczinski, "Role of Photoplethysmography in the evaluation of venous insufficiency.," *Bruit,* 1981.

[27] H. B. Abramowitz, L. A. Queral, W. R. Finn, P. F. Nora Jr, L. K. Peterson, J. J. Bergan and J. S. Yao, "The use of Photoplethysmography in the assessment of venous insufficiency: A comparison to venous pressure measurements.," *Surgery,* 1979.

[28] A. V. Oppenheim, R. W. Schafer and J. R. Buck, Discrete-time signal processing, Upper Saddle River: Prentice Hall, 1999.

[29] S. Butterworth, "On the theory of filter amplifiers," *Wireless Engineer,* vol. 7, pp. 536-541, 1930.

[30] G. J. Langewouters, A. Zwart, R. Busse and K. H. Wesseling, "Pressure-diameter relationships of segments of human finger arteries," *Clinical physics and physiological measurement,* vol. 7, no. 1, 1986.

[31] Y.-c. Fung, Biomechanics: Circulation, Springer, 1996.

[32] Y.-c. Fung, Biomechanics: Mechanical Properties of Living Tissues, Springer, 1993.

[33] W. A. Riley, R. W. Barnes, G. W. Evans and G. L. Burke, "Ultrasonic measurement of the elastic modulus of the common carotid artery: The Atherosclerosis Risk in Communities (ARIC) Study," *Stroke,* vol. 7, no. 23, pp. 952-956, 1992.

[34] Wikipedia; ProfBondi, "Continuous Noninvasive Arterial Pressure," 10 November 2012. [Online]. Available: http://en.wikipedia.org/wiki/Continuous_Noninvasive_Arterial_Pressure.

[35] E. Sackl-Pietsch, "Continuous non-invasive arterial pressure shows high accuracy in comparison to invasive intra-arterial blood pressure measurement," [Online]. Available: http://www.biopac.com/Manuals/nibp100d_white_paper.pdf.

[36] D. B. Wax, H.-M. Lin and A. B. Leibowitz, "Invasive and concomitant noninvasive intraoperative blood pressure monitoring: observed differences in measurements and associated therapeutic interventions.," *Anesthesiology,* vol. 115, no. 5, pp. 973-978, 2011.

[37] I. C. Jeong, S. O. H. Jae Il Ko and H. R. Yoon, "A new method to estimate arterial blood pressure using photoplethysmographic signal," in *EMBS'06. 28th Annual International Conference of the IEEE*, 2006.

[38] M. Cejnar, H. Kobler and S. N. Hunyor, "Quantitative photoplethysmography: Lambert-Beer law or inverse function incorporating light scatter," *Journal of biomedical engineering,* vol. 15, no. 2, pp. 151-154, 1993.

[39] V. C. Roberts, "Photoplethysmography--fundamental aspects of the optical properties of blood in motion.," *Trans. IMC,* vol. 4, pp. 101-106, 1982.